DETERMINATION OF SPIN STRUCTURES OF THE RARE EARTH ALLOYS BY NUCLEAR POLARIZATION TECHNIQUE

Yukio AOKI

1974

論文目録

大阪大学

報告番号	甲第1753号	氏名	青木征男

主論文

題名

Determination of Spin Structures of the Rare Earth Alloys by Nuclear Polarization Technique

(核整列法による希土類合金のスピン構造の決定)

参考論文

題名

Determination of the Semi-Cone Angle of Tb in Tb-Er Alloy by Nuclear Polarization Method

(核整列法による Tb-Er 合金中の Tb のセミコーン角度の決定)

J. Phys. Soc. Japan 36 (1974) 1703

日野谷重晴、伊藏順吉と共著

Contents

Synopsis

Single crystals of heavy rare earth alloys, $Y_{31}Tb_{69}$ and $Er_{84}Tb_{16}$, were cooled down to about 40 mK by heat conduction through a copper rod connected to an adiabatically demagnetized K-Cr alum salt. By slow neutron bombardment, small amounts of Tb^{159} had been transformed to radioactive Tb^{160} and the anisotropies of γ-rays emitted from polarized Tb^{160} nuclei were measured. Because the γ-ray anisotropy depends upon the spin structure, we could determine spin strucrures of these alloys by this method.

In the case of the $Y_{31}Tb_{69}$ alloy, the phase transition from spiral structure to ferromagnetic one under an external magnetic field was studied. The alloy did not transit below 10 KOe around 40 mK. We also measured magnetization curves of the alloy at 4.2 K and it was revealed that the alloy transited at 18 KOe in the first run but the critical field was reduced to a few KOe in the second and further runs. These results are consistent with the above nuclear polarization experiments but this strange phenomenon has not been explained theoretically.

In the case of $Er_{84}Tb_{16}$ alloy whose spin structure is conical at low temperature, the semi-cone angle of Tb ion, Θ_{Tb}, was determined to be $66^{\circ} \pm 4^{\circ}$ by the nuclear polarization technique. On the other hand, the semi-cone angle of Er ion, Θ_{Er}, is about 30° which was determined by means of neutron diffraction technique by A.H.Millhous et al. Then the semi-cone angles of Tb and Er ions are different from each other, that is, the structure is "a double cone structure". We made some simple calculations based on a model in which isotropic exchange integrals common to both the components of the alloys and one-ion anisotropies are assumed. Because many parameters which are not exactly known are necessary in the numerical calculation, it may be impossible to compute semi-cone angles of Tb and Er from the first principle. But it is

shown that for some restricted range of the numerical values of the parameters, a double cone structure which is compatible with the observed one is actually expected. The origin of the difference of the semi-cone angles of Tb and Er in the alloy is the large difference in the anisotropy energies of these two ions; the anisotropy energy minimum lies in the c-plane in Tb while it is along the c-axis in Er.

This is the first successful work to determine spin structures using nuclear polarization technique. The spin structure is determined by only γ-ray countings in this method. Then this technique is useful for alloy systems, namely the spin direction of minority atoms or ions are able to be determined "accurately and directly" with this technique, in contrast with the neutron diffraction technique and the spin echo method.

§1. Introduction.

In our laboratory, in order to perform nuclear polarization experiments low temperature equipments have been constructed in recent years. At the first, we have done experiments of the nuclear magnetic resonance on oriented nuclei (NMR/ON) and measured the field dependence of the nuclear spin lattice relaxation time of Co^{60} nuclei in the iron[1]. Secondly, single crystals of heavy rare earth metals and alloys have been studied with the nuclear polarization technique to know the magnetic structures of the alloys. The latter results will be reported in this thesis.

Magnetic structures of heavy rare earth metals and alloys which all have simple hexagonal structure in the paramagnetic phase have recently come to light by neutron scattering experiments, using single crystal samples, of the Oak Ridge National Laboratoy's groups. For example, the magnetic phase of terbium metals changes from paramagnetic structure to spiral one at 230 K, and from spiral one to ferromagnetic one at 221 K. Throughout the ordered phases, the moments lie in the c-plane. Erbium metals have more complex transitions, and at the lowest temperatures (i.e. below 20 K) they have conical structure whose semi-cone angle is 28.5°. Thus at low temperature the angle between the crystalline c-axis and the moment is 90° in terbium metals and 28.5° in erbium metals. The different angles in these metals come from the difference in the anisotropy energies about the c-axis. Then it is interesting whether the direction of the moments of the terbium atoms and that of the erbium atoms in erbium-terbium alloys are the same or different. In 1969 Millhous et al.[2] measured the spin structures of these alloys with the neutron diffraction technique. Their results showed that the alloys in which the terbium concentration is less than about 40 at.% have conical structure at low temperature. They measured the moments parallel to and perpendicular to the c-axis, which, for example in Er(90 at.%)-Tb(10 at.%) alloy, are 7.8 μ_B and

$4.6\mu_B$, respectively, at 4.2 K. From these values they determined the semi-cone angles of the average moment. By the neutron diffraction technique, it is difficult to determine the semi-cone angle of the minority terbium ions separately because of the poor resolutive power. On the other hand, because only the γ-rays emitted from radioactive Tb nuclei are detected in nuclear polarization experiments, it seems easy to determine the semi-cone angles of Tb ions, even if the concentration of Tb is quite small. First purpose of this thesis is the determination of the semi-cone angle of Tb ion in these alloys. It is necessary for the performance of the nuclear polarization experiments that there is appropriate radioactive isotopes whose nuclear spin is greater than 1/2, whose half life time is fairly long and which emitts suitable γ-rays. Tb^{160} nuclei satisfy these conditions. On the contrary, there is none of such erbium radioactive isotope. Thus, the semi-cone angles of only terbium ions can be measured by this method. Since the semi-cone angle of the terbium atoms was not determined by neutron diffraction technique, the experiments of nuclear polarization in these alloys seem very interesting.

Next the transition in yttrium-terbium alloys from spiral structure to ferromagnetic one under an external magnetic field will be considered. Koehler et al.[3] and Chield et al.[4] revealed that the yttrium-terbium alloys in which the terbium concentration is less than about 75 at. % have spiral structure at low temperature. It is expected that these alloys will make a transition from spiral structure to ferromagnetic one when an appropriate external magnetic field is applied and that this process can be observed by nuclear polarization technique as well as by magnetization measurements. The observation of this process is the second purpose of this thesis. We also measured the magnetization curves of the alloys in addition to the nuclear polarization experiments.

The samples on which we performed nuclear polarization experiments were studied at the same time by the usual spin echo methods by Dr. Sano and Mr. Shimizu and the nuclear hyperfine energies of the stable isotopes in these alloys were determined. These values will be used to analyze our experimental results. They also determined the semi-cone angles of Er and Tb ions in Er-Tb alloys. Contrary to the neutron scattering experiments, the spin echo methods have a merit that the semi-cone angle of each atom in the alloys can be determined independently, but to obtain numerical values it is necessary to assume that the electric field gradient produced by the 4f electrons of the parent ion is independent of the concentration of the alloy. On the other hand, in the nuclear polarization experiments the semi-cone angle is determined directly from the γ-ray anisotropic measurements. Thus the nuclear polarization technique is very suitable for the study of spin structure in some complicated system.

Nuclear polarization experiments have been done by many workers to investigate the nuclear properties and hyperfine interactions and often to determine temperatures. Perhaps none have done to determine the spin structures of magnetically ordered materials by this method, except Lebrance et al.[5] who observed the γ-ray anisotropies of Ho^{166m} nuclei in holmium single crystal. But they did not analyze fully their results. We believe that our measurements are first successful works in which the spin structures of the alloys are determined by nuclear polarization technique.

To determine the temperature of the sample, the degree of the nuclear polarization of Ir^{192} nuclei in a dilute Ir-Fe alloy attached to the sample was measured.

In next section, we calculate the anisotropic angular distributions of the γ-rays emitted from Tb^{160} nuclei in various magnetically ordered phases and from that Ir^{192} nuclei in the ferromagnetic iron alloy. These numerical calculations have been done with the NEAC series model 2200 computer in Osaka

University. These results are used to discuss our experimental results. In section 3, we explain the methods of the preparation of the single crystals and production of the radioactive Tb^{160} and Ir^{192} nuclei, and the experimental apparatus. In the last section we describe the experimental results and discussions.

§ 2 γ-ray angular distributions.

§ 2-1 General formulas of the γ-ray angular distributions.

Let us consider the nuclei which decay from a state of the nuclear spin J into a state of the nuclear spin J_1 emitting a single γ-ray with the angular momentum L. We denote this process as $(J \xrightarrow{L} J_1)$. Then the angular distribution of γ-rays emitted from the nuclei polarized in one direction is written, following the Steenberg's work[6], by

$$I(\theta) = \sum_{m=-J}^{J} W_m(T) \cdot I_m(\theta) \Big/ \sum_{m=-J}^{J} W_m(T) , \qquad (1)$$

where

$$I_m(\theta) = 1 + \sum_{K:\text{even}} a_K(L) \cdot S_K(J, J_1, L) \cdot \Pi_K(m, J)\, P_K(\cos\theta) . \qquad (2)$$

K is restricted to $K \leq 2L$ and $K \leq 2J$, m is the z-component of the nuclear spin J, $W_m(T)$ is the population of nuclei in the m-th level which depends on absolute temperature T, $P_K(\cos\theta)$ is the k-th Legendre polynomial and is normalized in the sense that $P_K(1) = 1$ and θ is the angle between the direction of the γ-ray emission and the axis of polarization. The expressions of $a_K(L)$, $S_K(J, J_1, L)$ and $\Pi_K(m, J)$ are given by Steenberg[6]. Next, in the case of the successive emissions of γ-rays which are represented with $(J \xrightarrow{L_1} J_1 \xrightarrow{L_2} J_2)$, Eq.(2) is rewritten as follows;

$$I_m(\theta) = 1 + \sum_{K:\text{even}} a_K(L_2) \cdot S_K(J_1, J_2, L_2) \cdot S_K(J, L_1, J_1)\, \Pi_K(m, J) \cdot P_K(\cos\theta) . \qquad (3)$$

K is now restricted to $K \leq 2L_2$, $K \leq 2J$ and $K \leq 2J_1$. Using Eq.(3), Eq. (1) is rewritten

$$I(\theta) = 1 + \sum_{K:\text{even}} B_K(T) \cdot U_K \cdot P_K(\cos\theta) , \qquad (4)$$

where

$$B_K(T) = \sum_{m=-J}^{J} W_m(T) \cdot \Pi_K(m, J) \Big/ \sum_{m=-J}^{J} W_m(T)$$

$$U_K = a_K(L_2) \cdot S_K(J_1, J_2, L_2) \cdot S_K(J, L_1, J_1)$$

Above results are normalized in the sense that $I(\theta)=1$ for high enough temperature where the nuclei is unpolarized. Usually we measure γ-rays at low temperature (30 mK or so) where nuclei are partially polarized, and the counting rate at this temperature is divided by that measured at high temperature($T \simeq 1K$). This ratio gives the experimental $I(\theta)$ value. These $I(\theta)$values (hereafter we write as "the γ-ray anisotropy") tell us $B_K(T)$ values when U_K are known. From these $B_K(T)$ values we can get the knowledge about the effective field on the nuclei in a ferromagnetic sample when T is known or absolute temperature T when the effective field is known, because $B_K(T)$ is the function of these.

When the magnetic structure is simply antiferromagnetic, the above formulas equally holds, but when the magnetic structure is more complicated, $P_K(\cos\theta)$ in Eq.(4) should be properly modified. In the case of the conical structure whose semi-cone angle is α, $P_K(\cos\theta)$ in Eq.(4) should be modified to $P_K(\cos\theta)\cdot P_K(\cos\alpha)$, where θ is the angle between the axis of the cone and direction of the γ-emission. Thus, the measurements of the γ-ray anisotropy tell us the semi-cone angle if $B_K(T)$ and U_K in Eq.(4) are known. In this sense, the nuclear polarization experiments can give some knowledge on the spin structures. In the following subsections, details on the γ-ray anisotropy of Tb^{160} and Ir^{192} nuclei are discussed.

§2-2 γ-ray angular distributions of the Tb^{160} nuclei.

The abbreviated decay scheme of the Tb^{160} nuclei is given in Fig.1 and its energy spectrum measured in our laboratory with a 2 in. x 2 in. NaI(Tl) scintillation counter is shown in Fig.2. The decay scheme of the Tb^{160} nuclei is very complex but we concern only 1178.1 KeV, 1272.0 KeV and 298.5 KeV γ-rays whose γ-ray anisotropies are larger than others and transition schemes are the same, represented by $(3 \xrightarrow{1} 2 \xrightarrow{1} 2)$. We can easily calculate the angular distribution of this transition at the limit of the absolute zero

temperature (T=0) where all $W_m(0)$ equal zero except $W_J(0)$ or $W_{-J}(0)$, that is

$$\begin{aligned} I(\theta) &= I_J(\theta) \\ &= 1 - \frac{1}{2} P_2(\cos\theta) \\ &= \frac{5}{4} - \frac{3}{4}\cos^2\theta \end{aligned} \qquad (5)$$

We get easily that $I(0)=0.5$ and $I(\pi/2)=1.25$. These results mean that the γ-ray counting number at $\theta=0$ is much less than that at $\theta=\pi/2$.

The above results are very simple, but unfortunately there are other γ-rays which have nearly same energies as those of the above γ-rays and decay through other schemes, for example, 309.6 KeV γ-ray which is very close to 298.5 KeV one. Since these two can not be resolved by the NaI(Tl) scintillation counter and since the transition scheme of 309.5 KeV γ-ray is $(3 \xrightarrow{1} 2 \xrightarrow{1} 3)$, the γ-ray angular distribution is different from that of 298.5 KeV γ-rays. Though the intensity of the 309.6 KeV γ-rays is much weaker than that of 298.5 KeV γ-rays, the anisotropy in the sum of these unresolved γ-rays is slightly different from that given by Eq.(5), when the weighted average is calculated. Also, in the case of 1178.1 KeV and 1272.0 KeV γ-rays which are unresolved by our scintillation counter, there are other three γ-rays which we must take into account, that is 1115.0 KeV, 1200.0 KeV and 1312.0 KeV γ-rays. The transition schemes and U_2 values for all these γ-rays listed in Table I. The signs of U_2 show that the γ-ray anisotropies of three main transitions are given by Eq.(5) and those of other minor ones have opposite signs. Then the anisotropies of the unresolved γ-ray peaks are smaller than that given by Eq.(5). Using U_2 values and transition probabilities in Table I, we can calculate the anisotropies of these peaks at the limit of the absolute zero temperature (T=0). The results are as follows;

for the higher than 1.1 MeV peaks (which are the sum of the 1115.0, 1178.1, 1200.0, 1272.0 and 1312.0 KeV γ-rays);

$$I(0) = 0.7267 \quad , \quad I(\pi/2) = 1.1366 \,,$$

for the 300 KeV peaks (which are the sum of the 309.6 KeV and 298.5 KeV γ-rays);

$$I(0) = 0.5486 \qquad I(\pi/2) = 1.2257$$

Let us consider a finite temperature case. When only the nuclear Zeeman energy and the electric quadrupole energy are considered, the energy of the nuclear m substate is

$$E_m = -\gamma_n \hbar H_0 m + \frac{e^2 q Q}{4J(2J-1)} (3m^2 - J(J+1)) \qquad (6)$$

We here assume that the principal axis of the electric field gradient is parallel to the direction of the electronic magnetization and also the electric quadrupolar tensor is axially symmetric. Then, the population of the nuclei at the m substate is represented as

$$W_m(T) = \exp(-E_m/kT) \Big/ \sum_{m=-J}^{J} \exp(-E_m/kT)$$

The values of $\gamma_n \hbar H_0$ and e^2qQ of the Tb^{159} nuclei in ferromagnetic Tb metal are measured by the spin echo method in our laboratory[7] i.e. $\gamma_n \hbar H_0 =$ 3120 MHz and $e^2qQ = 1347$ MHz. Since the γ value of Tb^{159} nuclei is 9.6540 MHz/10^4 Oe and that of Tb^{160} nuclei is 4.0648 MHz/10^4 Oe, $\gamma_n \hbar H_0$ for Tb^{160} nuclei is calculated to be 1308.6 MHz. Next, the value of Q of the Tb^{160} nuclei was determined to be 3.0 barns by Easley et al.[8] and it is already known that the value of Q of the Tb^{159} nuclei is 1.34 barns, then the value of e^2qQ of the Tb^{160} nuclei is estimated to be 3016 MHz. Using these values, we can calculate γ-ray anisotropies of the Tb^{160} nuclei in the ferromagnetic structure.

Next we consider the case of the conical spin structure of the erbium-terbium alloys. Let us see Fig.3, where we take the polar axis as the crystalline c-axis, the angular coordinates of a nuclear spin as α and φ (α is the semi-cone angle) and the observation direction as β and φ'. Ψ is

an angle between a nuclear spin and the observation direction. When the turn angle of the conical structure is not an integral of 2π, which may be generally the case, the nuclear spins are distributed such as φ is uniform over 2π and the γ-ray anisotropy observed by our experiment corresponds tothe case where the average of $P_K(\cos\Psi)$ over φ is taken instead of $P_K(\cos\theta)$ in Eq.(4), or

$$\frac{1}{2\pi}\int_0^{2\pi} P_K(\cos\Psi)\,d\varphi$$
$$= \frac{1}{2\pi}\int_0^{2\pi}\sum_{l=-k}^{k}\frac{(k-|l|)!}{(k+|l|)!}\cdot P_K^{|l|}(\cos\alpha)\cdot P_K^{|l|}(\cos\beta)\cdot e^{il(\varphi-\varphi')}\,d\varphi$$
$$= P_K(\cos\alpha)\cdot P_K(\cos\beta) \quad .$$

Here we used the addition theorem of the Legendre polynomials. Since $B_K(T)$ and U_K in Eq.(4) are the same as those in the ferromagnetic case, $I(\alpha,\beta)$ is given by

$$I(\alpha,\beta) = 1 + \sum_{K:\,even} B_K(T)\cdot U_K\cdot P_K(\cos\alpha)\cdot P_K(\cos\beta) \quad , \qquad (8)$$

If $\alpha = 0$ (the ferromagnetic case), $P_K(\cos\alpha)$ becomes unity and Eq.(8) is reduced to the Eq.(4), that is, $I(0,\beta) = I(\beta)$. If $\alpha = \pi/2$ (the spiral case), we obtain $P_K(\cos\alpha) = -1/2$, and with the subscript S_p for the spiral structure,

$$I_{S_p}(\beta) = I(\pi/2,\beta)$$
$$= 1 - \frac{1}{2}\sum_{K:\,even} B_K(T)\cdot U_K\cdot P_K(\cos\beta) \quad . \qquad (9)$$

We note that $I(\alpha,\beta)$ is unchanged by the exchange α and β. This result is very important. If the semi-cone angle α satisfies $P_K(\cos\alpha) = 0$, then $I(\alpha,\beta)$ becomes unity whatever β and T are. Some results of calculations of Eq.(8) and Eq.(9) are shown in Fig.4 and 5. The $\gamma_n\hbar H_0$ values of Tb^{159} nuclei in Tb-Er and Tb-Y alloys are measured in our laboratory by spin echo method. For example the $\gamma_n\hbar H_0$ value in Er-10 at.% Tb alloy is 3182 MHz and this value is used instead of the value in the ferromagnetic terbium metal (i.e. 3120 MHz) in the above calculations.

§2-3 γ-ray angular distribution of the Ir^{192} nuclei.

We can know $B_K(T)$ from the measurements of the γ-ray anisotropy since U_K values can be calculated if the nuclear transition scheme is known. $B_K(T)$ is a known function of the absolute temperature T and nuclear Zeeman energies when e^2qQ can be neglected. By the measurement of the γ-ray anisotropy of the nuclei whose nuclear transition scheme and Zeeman energies are accurately known, we can determine the absolute temperature. For the determination of the temperature, we used Ir^{192} nuclei in the iron (Fe-0.3 at.% Ir), firstly because the γ-ray anisotropy changes sensitively with the temperature in the range from 20 mK to 50 mK due to fairly large value of the Zeeman energy, and secondly because the half life time of the Ir^{192} nuclei is fairly long ($T_{\frac{1}{2}}$ = 74.2 days). The abbreviated decay scheme of the Ir^{192} nuclei is given in Fig.6. We use the 468.1 KeV peak for the temperature determination. Weak γ-rays of the energy 484.6 KeV overlap to this peak and this mixing should be taken into account for the calculation of the γ-ray anisotropy (see Fig.7). This effect is similar to the case of Tb^{160} nuclei discussed already. In contrast with the Tb^{160} case, U_2 and U_4 term are necessary for the calculation because of the electric quadrupole nature of the transitions in Ir^{192} nuclei. These values are also given in Table I. The $\gamma_n\hbar H_0$ value of Ir^{192} nuclei in the iron was determined as 407.54 MHz by Reid et al.[9], using nuclear polarization technique. Neglecting the second term in Eq.(6), we calculate the γ-ray anisotropy for the 468.1 KeV peak, and the results are shown in Fig.8. This curve is used for the determination of the temperature.

§3 Experimental procedures.

§3-1 Sample preparations.

The Nigh's methods[10] were applied to the growth of the single crystals of heavy rare earth alloys. First we cut the ingots of the pure metals of 99.8% purity in appropriate masses and then melt them with an argon arc furnace overturning about five times to homogenize the sample. To prevent distillations in the following process, especially for the erbium alloys, the alloy was enclosed with argon gas of appropriate pressure in a quartz or an alumina tube. Then it was annealed in a siliconit furnace at a temperature somewhat below the melting point for a few days. The formation of the single crystal was checked and then the crystalline axes were determined by reflected Laue patterns of X-rays. The single crystal was cut in a desired shape and polished. The final shape of the most samples was a thin disk of 4 mm x 2 mm x 0.2 mm in which the b-axis was parallel to the longest side and the c-axis was perpendicular to the surface of the disk. We got successfully Y(31.4 %)-Tb(68.6 %) and Er(83.8 %)-Tb(16.2 %) single crystals.

Next step of the sample preparation is the creation of radioactive nuclei. We sent the single crystal samples to the Japan Atomic Energy Research Institute in Tokai Village, Ibaragi Prefecture. The sample enclosed in a quartz tube was put into the reactor and irradiated with slow neutrons to produce Tb^{160} active nuclei of a few μCi.

The active iridium nuclei Ir^{192} in iron were also obtained by the neutron irradiation of Fe-0.3 at. % Ir alloy.

§3-2 Experimental apparatus.

Since most parts of the experimental apparatus and procedure of adiabatic demagnetization are the same as one described by Dr.Kohzuki[11], we explain them briefly.

Very low temperature (30 mK or so) was obtained by the adiabatic demagnetization of chromium potassium alum. It is very important in these experiments to cool the alloy sample and to keep its temperature low enough for a long time. For these purposes, our cooling system was designed as follows; The sample was soldered with indium soft solder at one end of a copper rod and many copper wires were soldered with $Cd_{40}Bi_{60}$ soft solder at the other end of that copper rod. The chromium potassium alum was crystallized around these copper wires in order to have a good thermal contact between the alum and copper wires. The copper rod and alum were enclosed in a thermal shield which is cooled down to about 0.1 K with another alum. The thermal shield was supported by a bakelite rod in a vacuum cell which was immersed in liquid helium. By this procedure the sample was cooled to the lowest temperature (30 mK or so) about 30 minute after the field was demagnetized and then the raising rate of temperature was about 1 mK/hr.

The initial conditions of the adiabatic demagnetization were about 1.2 K and 18 KOe. A superconducting magnet was used to study the transition of the Y(31.4 at. %)-Tb(68.6at. %) alloy. Also, this magnet was used to saturate magnetically the iron-iridium thermometer. The γ-rays were detected with two NaI(Tl) scintillation counters. One of these counters was set parallel to the b- and the other to the c-axis of the sample. The signals from the counters were analyzed by a pulse hight analyzer (PHA) and energy spectra of the γ-rays emitted in the two direction were obtained. The 300 KeV and the higher-than-1.1 MeV peaks of the Tb^{160} γ-rays were used to obtain the nuclear polarization as described earlier.

§4 Experimental results and discussion.

§4-1 Thermometer.

It is very difficult to measure temperature accurately at very low temperature. In the adiabatic demagnetization experiments, the paramagnetic susceptibility of the demagnetized salt is usually measured to know its temperature. In our experiments, we always measured the paramagnetic susceptibility of the chromium potassium alum by the usual A.C. Hartshon bridge method[12]. This value tells us the magnetic temperature T^*, then we can know the absolute temperature T because the relation between T^* and T is known[13),14)]. But the relation is not so accurate at very low temperature ($\sim$20 mK) and moreover the temperature of the sample may not be always the same as that of the alum. Then it is needed to know the temperature of the sample accurately and directly.

It was already noted that the γ-ray anisotropic distribution emitted from aligned nuclei whose nuclear properties are well known tells us temperature. For this purpose the 470 KeV peak (which are the sum of the 468 KeV and 485 KeV γ-rays) of the Ir^{192} in Fe-0.3 at. % Ir alloy was used. The activated Fe-0.3 at. % Ir alloy was soldered to the copper rod of the cooling system together with the sample when its use was desired. The temperature T_γ can be determined easily from the measured γ-ray anisotropies using Fig.8(a). It was assured from these experiments that the temperature measured with the Fe-0.3 at.% Ir alloy thermometer, T_γ, nearly coincided with the temperature measured with the paramagnetic susceptibility, T_χ. Therefore, in most experiments the temperature of the sample was determined by the paramagnetic susceptibility measurements of the alum.

§4-2 Y(31.4 at.%)-Tb(68.6 at.%) alloy.

i) Magnetization measurements.

We measured the magnetization curves of the Y(31.4 at.%)-Tb(68.6at.%) single crystal alloy using a magnetic balance at 77 K and 4.2 K. It is well known that at zero external field the magnetic structure is spiral at these temperatures[3),4)] and when the external field is applied along the b-axis, the transition to ferromagnetic structure occurs most easily.

The results of the experiments show that at 77 K there is a hysteresis in the transition field H_c from spiral to ferromagnetic structure (7.5 KOe for increasing and 5.5 KOe for decreasing field). The magnetic moment amounts to 290 cgsemu/Tb g at 10 KOe (the saturation moment of pure terbium single crystal is 328 cgs emu/g[15)] and it is calculated that it becomes 295 cgs emu/g under the above conditions). Thus, we conclude that the alloy makes a transition from spiral to ferromagnetic structure under the external field at 77K. It was found that a fairly long relaxation time is needed for the transition, namely when the applied field is increased (or decreased) about 500 Oe around the transition field, the force acting on the alloy in the magnetic balance measurement increased (or decreased) gradually and did not come to an exact equilibrium even after 10 minute.

In contrast with the results at 77 K, the experimental results at 4.2 K were much more complex as shown in Fig.9. When the external field was applied in a virgin sample, the transition field is 18 KOe in the first run and thereafter it is always 4 KOe in decreasing the field and 6 KOe in increasing the field. This means that the transition field for the virgin sample is very high (18 KOe) but it becomes lower with a hysteresis (6 KOe and 4 KOe) in succeeding cycles. The same phenomena was observed in the magnetostriction at 4.2 K by Mr.Hinotani[16)] in our Laboratory.

Next, we measured temperature dependence of the magnetization. The result is shown in Fig.10. When the sample was cooled down to liquid helium temperature first without appling an external field and then a magnetic

field of 10 KOe was applied, the sample was still in conical phase. When the temperature of the sample was raised, it was found that the transition to ferromagnetic state occured at 20 K in increasing temperature, but in return cycle, no transition occured down to 4.2 K, indicating that the sample was still in ferromagnetic state. These results will be discussed in connection with the nuclear polarization studies.

ii) Nuclear polarization experiments.

We measured the magnetic field dependence of the γ-ray anisotropies I_b and I_c, in the directions along the b- and c-axes, respectively. The field, parallel to the b-axis, was increased up to 13 KOe but I_b and I_c were independent of the field strength within the experimental error. This fact means that the magnetic structure of the alloy remains the same up to this field strength at verly low temperature.

The experimental results are shown in Table II(a). The temperature dependence of the γ-ray anisotropies were already calculated for the various magnetic structures as explained in the chapter 2. The calculated temperatures T_γ, using the above measured anisotropies I_b and Fig.5, are nearly equal to the temperature T_χ measured by the susceptibility of the alum, assuming the magnetic structure is spiral. On the other hand, if the ferromagnetic structure aligned along the b-axis direction is assumed, the calculated temperature T_γ using I_b is much higher than T_χ ($T_\gamma \sim 115$ mK) which is very improbable.

Thus it is concluded that the magnetic structure of this alloy is spiral at zero external field and remains the same up to 13 KOe at this temperature. These results are consistent with the magnetization measurements described earlier.

iii) Summary.

Magnetization measurements at 77 K and 4.2 K and nuclear polarization experiments around 40 mK were performed for the Y(31.4 at.%)-Tb(68.6 at.%) alloy to investigate the transition from the spiral structure to the ferromagnetic one under an external magnetic field. The transition field is several KOe at 77 K, while at 4.2 K the transition field is 18 KOe in the first run, but in successive runs it becomes several KOe which is somewhat lower than that at 77 K. These results are summarized in Fig.11. By the nuclear polarization experiments at about 40 mK, it was found that the magnetic structure remained spiral up to the external field strength of 13 KOe being consistent with the results of magnetization measurements.

It looks like that first the magnetic moments are pinned by some unknown reasons and the transition field becomes very high in the first run at lower temperature. But once the transition to the ferromagnetic structure occurs, the pinning disappears and never appears again. As for the origin of the pinning, we can imagine something, for example, lattice defect, magnetic striction and so on. But the strange magnetic behavier at low temperatures of this alloy can not be well explained at the present stage.

§4-3 Er(83.8 at.%)-Tb(16.2 at.%) alloy.

i) Experimental results.

It is the purpose in this experiments to determine the semi-cone angle of the Tb ion θ_{Tb} in the Er(83.8 at.%)-Tb(16.2 at.%) single crystal alloy. The γ-ray anisotropies I_b and I_c of the 300 KeV and higher-than-1.1 MeV γ-ray photons of Tb^{160} were measured. The temperature of the sample was determined by the measurements of the susceptibility of the adiabatically demagnetized salt. The results are summarized in Table II(b). The semi-cone angle of the Tb ion θ_{Tb} was determined from the these results are shown in Fig.12. The errors in θ_{Tb} come mainly from the errors in the temperature measurements and the γ-ray anisotropies. The temperature of the sample increases monotonically and changed by a few mK during the γ-ray counting which is shown in Table II(b). We calculated I corresponding to the middle temperature and the results are shown in Fig.12. Concerning the error in I_{exp}, the statiscal error arising from γ-ray counting is fairly small, but in addition to it there are several errors arising from experimental set up, namely the directional difference between the crystal axis and the counter direction, channel drifts of the PHA and so on. Though these errors can not be estimated quantitatively, we estimated the error in I_{exp} to be about ± 1 %. Fig.12 shows this process and the values of θ_{Tb} with estimated error are summarized in Table II(b). The four independent values θ_{Tb} determined from $I_b = I(\theta_{Tb}, \pi/2)$ and $I_c = I(\theta_{Tb}, 0)$ for the 300 KeV and higher-than-1.1 MeV γ-ray photons coincide within the error. This good coincidence supports the validity and accuracy of our experiments. We conclude that $\theta_{Tb} = 66^\circ \pm 4^\circ$. This result is consistent with the results obtained by the spin echo measurements[17].

Because the nuclear properties of Tb^{160} are well known, it seems that there is no ambiguity in the calculation of the γ-ray anosotropy emitted from the polarized nuclei. Thus the semi-cone angle θ_{Tb} in this alloy was most directly determined by these measurements. This is largely different from the spin echo

method which needs some assumptions about the origin of the electric field gradient, q. Moreover θ_{Tb} is obtained independently of θ_{Er} in contrast with the neutron scattering technique. Thus, in favorable cases, nuclear polarization technique is very suitable for the investigation of the magnetic structure of some complex system.

These results were already reported [18].

ii) Double cone structure.

The above result means that the semi-cone angle of the Tb ion in the Er(83.8 at.%)-Tb(16.2 at.%) alloy is about 66°. According to the neutron scattering experiments[2], the spin structure of the alloy is conical at very low temperature and the semi-cone angle of the average moment (that is, the concentration average of Er and Tb) is about 30°, or, because the concentration of the Er ion is much larger than that of Tb ion, the semi-cone angle of Er ion is approximately of this magnitude. Then it is concluded that the spin structure of this alloy is "a double cone structure", namely the Er and Tb ion have different semi-cone angles. This is physically explained as follows. Er and Tb ions have proper large magnetic anisotropy energy, and the easy direction of Tb ion in Tb metal is the b-axis while that of Er ion in Er metal is the c-direction. In the alloy, each ion still has a proper anisotropy energy which is, however, slightly affected by the surrounding dislike ions. This proper large anisotropy energies cause that each ion has a different semi-cone angle.

Now we consider theoretically about the possibility of the double cone structure in detail. Miwa et al.[19] discussed magnetic orderings in the rare earth metals and calculated its energies with various ordered states. The energy in the cone state is given, following Miwa et al.[19], by

$$E(\theta)/N = -J(Q)\cdot S^2 - \{J(0) - J(Q)\} S^2 \cos^2\theta + D\cdot P_2(\cos\theta) + E\cdot P_4(\cos\theta) + F\cdot P_6(\cos\theta) \qquad (1)$$

where θ is the semi-cone angle, N is number of the ions, S is the components of the spin along the direction of the total angular momentum, or the spin itself in heavy rare earths, $J(q)$ is the Fourier transform of the exchange integral, Q is the turn angle, namely $J(q)$ has a maximum at $q=Q$, and D,E and F are the second, fourth and sixth coefficients of the anisotropy energy respectively. We calculate the energy in the double cone state of the alloy and the result is as follows;

$$
\begin{aligned}
E(\theta_1,\theta_2)/N = & -c^2 S_2^2 \left\{ J_{22}(Q) + \left[J_{22}(0) - J_{22}(Q) \right] \cos^2\theta_2 \right\} \\
& -(1-c)^2 S_1^2 \left\{ J_{11}(Q) + \left[J_{11}(0) - J_{11}(Q) \right] \cos^2\theta_1 \right\} \\
& -2c(1-c) S_1 S_2 \left\{ J_{12}(0)\cos\theta_1\cos\theta_2 + J_{12}(Q)\sin\theta_1\sin\theta_2 \right\} \\
& + c\left\{ D_2 P_2(\cos\theta_2) + E_2 P_4(\cos\theta_2) + F_2 P_6(\cos\theta_2) \right\} \\
& + (1-c)\left\{ D_1 P_2(\cos\theta_1) + E_1 P_4(\cos\theta_1) + F_1 P_6(\cos\theta_1) \right\} ,
\end{aligned}
\tag{2}
$$

where subscript 1 means the erbium ion and 2 means the terbium ion and c is the concentration of the terbium ion. In a simple theory of RKKY interactions, it can be assumed that $J_{11}=J_{12}=J_{22}$. If the cone state is stable, the semi-cone angle of the Er and the Tb ion, θ_1 and θ_2, are determined by solving simultaneous equations,

$$
\frac{\partial E(\theta_1,\theta_2)}{\partial \theta_1} = 0 \quad \text{and} \quad \frac{\partial E(\theta_1,\theta_2)}{\partial \theta_2} = 0 \tag{3}
$$

Although the values of $J(0)$, $J(Q)$, D_i, E_i and F_i $(i=1,2)$ in this alloy are not exactly known, we can get θ_1 and θ_2 where $28.5^\circ < \theta_1 < \theta_2 < 90^\circ$ if we assume appropriate values for these. This means that it is possible theoretically that the semi-cone angle of the Tb ion is different from that of the Er ion. In the next subsection, taking Kasuya's calculations into acount, we will try to discuss the values of $J(0)$, $J(Q)$, D_i, E_i and F_i $(i=1,2)$ which are consistent with the experimental results.

iii) Calculation of exchange and crystalline field parameters.

Now we discuss about parameters J, D, E and F. Crystalline field parameters D, E and F for heavy rare earth metals were discussed and calculated by Kasuya[20] assuming the point charge model. Also, the exchange parameter J in pure heavy rare earth metals were discussed and estimated by him. These values in pure Er and Tb metals are listed in Table III (from now on we refer these values as the K-values).

In the case of Er, neutron scattering experiments on spin waves have been done by Nicklow et al.[21] and isotropic and anisotropic exchange constants were determined. However, it seems rather difficult to infer these constants in alloys only from the values for pure Er metal and also to obtain the value of semi-cone angles by a simple calculation taking isotropic and anisotropic exchange interactions into account. Therefore, for a phenomenological interpretation of a double-cone structure, we proceed our discussions following a simple expression of energy as given by Eq.(2).

First we consider the case of the pure Er metal. In this case Eq.(2) becomes Eq.(1) and equation

$$\frac{\partial E(\theta_1)}{\partial \theta_1} = 0 \qquad (4)$$

must be satisfied by the value of θ_1 which is determined experimentally, or $\theta_1 = 28.5^\circ$. From Eq.(1) and (4), we get

$$A + B\cos^2\theta_1 + C\cos^4\theta_1 = 0 \qquad (5\text{-a})$$

where

$$A = \left[S_1^2 \{J(Q) - J(0)\} + \frac{3}{2} D_1 \right] / F_1 - \frac{15}{2} \frac{E_1}{F_1} + \frac{105}{8} \qquad (5\text{-b})$$

$$B = \frac{35}{2} \frac{E_1}{F_1} - \frac{315}{4} \qquad (5\text{-c})$$

$$C = \frac{693}{8} \qquad (5\text{-d})$$

Since θ_1 and S_1 are known ($\theta_1 = 28.5^\circ$, $S_1 = 1.5$), Eq.(5-a) is a function of $\{J(Q) - J(0)\}/F_1$, D_1/F_1 and E_1/F_1. If we assume two of these, the rest can be determined.

Next step is a case of the alloy. Let us consider an $Er_{1-c}Tb_c$ alloy in which the terbium concentration, c, is only a few. Taking terms which depend on θ_2 and neglecting c^2 terms, Eq.(2) is reduced to

$$E_2(\theta_2)/N = -2c S_1 S_2 \left[J(0) \cos\theta_1 \cos\theta_2 + J(Q) \sin\theta_1 \cdot \sin\theta_2 \right] + c \left[D_2 P_2(\cos\theta_2) + E_2 P_4(\cos\theta_2) + F_2 P_6(\cos\theta_2) \right] \quad (6)$$

We will seek for relations between J, D, E and F which satisfy Eq.(5-a) and in which $E_2(\theta_2)$ becomes minimum around $\theta_2 \simeq 66^\circ$. If we use the K-values, Eq.(5-a) does not be satisfied. Then, E_1/F_1 and $J(Q) - J(0)$ are changed from the K-values, satisfing Eq.(5-a). Before calculations of Eq.(6) as a function of θ_2, D_2, E_2 and F_2 must be known and also J(Q) and J(0) must be known separately. Then we have three assumptions;

(1) the ratio $J(Q)/J(0)$ is the same as the K-values, that is,

$$J(Q)/J(0) = 5.508/3.424 = 1.609, \quad (7)$$

(2) the ratio of D_2/D_1, E_2/E_1 and F_2/F_1 are also the values which are calculated from the K-values, that is,

$$\frac{D_2}{D_1} = \frac{\bar{V}_2^\circ(Tb)}{\bar{V}_2^\circ(Er)} \cdot \frac{v_2^\circ(Er)}{v_2^\circ(Tb)} = \frac{9.77}{-4.20} \cdot \frac{683}{580} = -2.739$$

$$\frac{E_2}{E_1} = \frac{\bar{V}_4^\circ(Tb)}{\bar{V}_4^\circ(Er)} \cdot \frac{v_4^\circ(Er)}{v_4^\circ(Tb)} = \frac{-0.818}{-0.618} \frac{655}{730} = 1.184 \quad (8)$$

$$\frac{F_2}{F_1} = \frac{\bar{V}_6^\circ(Tb)}{\bar{V}_6^\circ(Er)} \cdot \frac{v_6^\circ(Er)}{v_6^\circ(Tb)} = \frac{-0.101}{0.775} \frac{283}{280} = -0.1317,$$

(3) $F_1 = 0.775 \times 10^{-15}$ erg (the K-value). (9)

From Eq.(5-a) we can determine some reasonable combination values of $\{J(Q) - J(0)\}/F_1$, D_1/F_1 and E_1/F_1. From these values, J(Q), J(0), D_2, E_2 and F_2 are obtained using above three assumptions. Then, θ_2 dependence of $E_2(\theta_2)$ can be calculated and we obtaine $\theta_{2\,min}$ in which $E_2(\theta_2)$ becomes minimum. Some these calculated results are shown in Table IV. When E_1/F_1 is assumed to be -0.7974 which is the same as the K-values, $\theta_{2\,min}$ is equal to 60° which

is almost independent of the exchange energy $J(Q)$ and $J(0)$. When $E_1/F_1 = -0.3987$, the situation is almost the same as the above case. These $\theta_{2\ min}$ are quite equal to the experimental value, $\theta_{Tb} = 66^\circ \pm 4^\circ$. On the other hand, if $E_1/F_1 = -1.595$, $\theta_{2\ min}$ largely depends on the exchange energy and it increases as the exchange energy does. When $J(Q) - J(0) = 2.085 \times 10^{-15}$ erg which is obtained using the K-values, $\theta_{2\ min}$ becomes 53°. This value is less than the experimental value, $\theta_{Tb} = 66^\circ \pm 4^\circ$. In conclusion, the double cone structure is realized theoretically, if some appropriate exchange and crystalline field parameters are assumed. These parameters, of cause, restricted within some values.

§4-4 Conclusion.

Nuclear polarization technique is firstly used to analyze a spin structure of the alloy, Er(83.8 at.%)-Tb(16.2 at.%) alloy, and the semi-cone angle of the Tb ion in the alloy is successfully determined to be $66^{\circ} \pm 4^{\circ}$. This technique is able to apply for any metals and insulators and it has some merits, namely, even if a sample is constituted with many kinds of atoms and some of them have a little composition, the spin direction of each atom can be determined respectively and directly from only the γ-ray countings. But this technique needs, at least, one isotope which emits appropriate γ-ray photons, then applicable samples are limitted a little.

Acknowledgements

I would like to express my sincere thanks to Professor J.Itoh for his continuous guidances and encouragements and also Professor K.Asayama for his kind encouragements.

It is my pleasure to thank Dr.M.Aiga and Mr.S.Hinotani, who are competent members in our nuclear polarization experimental group, for their kind co-works and valuable discussions.

I would also like to express my deep thanks to Dr.Mishima of Hiroshima University for his technical advices about the single crystal growth and Professor Kiritani and Dr.Miyoshi in our depertment for their kind advices about analyses of X-ray diffraction patterns.

The magnetization measurements have been done by the courtesy of Professor Haseda, Professor Tasaki and Dr.Amaya in our department, to whom I wish to express my deep thanks.

Finally, thanks are also due to Dr.S.Kohzuki and Mr.N.Yamashita, who were competent members in our group, for their kind co-works and grateful discussions during the construction of our low temperature equipment.

Reference

1) S.Kohzuki, Y.Aoki, N.Yamashita and J.Itoh; J.Phys.Soc.Japan 32(1972) 1678

2) A.H.Millhouse and W.C.Koehler; Intern.J.Magnetism 2 (1971) 389

3) W.C.Koehler, H.R.Child, E.O.Wollan and J.W.Cable; J.Appl.Phys.34(1963)1335

4) H.R.Child, W.C.Koehler, E.O.Wollan and J.W.Cable; Phys.Rev. 138 (1965) A1655

5) M.A.R.Leblance and W.T.Sommer; Low Temp.Phys (LT8) (1963) pp432-433

6) N.R.Steenberg; Proc.Phys.Soc. 65 (1952) 791

7) N.Sano and J.Itoh; J.Phys.Soc.Japan 32 (1972) 95

8) W.C.Easley, J.A.Barcley and D.A.Shirley; Phys.Rev. 170 (1968) 4

9) P.G.E.Reid, M.Sott and N.J.Stone; Nuc.Phys. A129 (1969) 273

10) H.E.Nigh; J.Appl.Phys. 34 (1963) 3323

11) S.Kohzuki; thesis:Osaka University (1972)

12) H.B.G.Casimir, W.J.De Haas and D.De Klerk; Physica 6 (1939) 241

13) E.Ambler and R.P.Hudson; Phys.Rev. 95 (1954) 1143

14) B.Bleany; Proc.Roy.Soc; A204 (1950) 216

15) D.E.Hegland, S.Legvold and F.H.Spedding; Phys.Rev; 131 (1968) 158

16) S.Hinotani; Master thesis: Osaka University (1974)

17) K.Shimizu; Master thesis: Osaka University (1973)

18) Y.Aoki, S.Hinotani and J.Itoh; J.Phys.Soc.Japan 36 (1974) 1703

19) H.Miwa and K.Yoshida; Prog.Theort.Phys. 26 (1961) 693

20) G.T.Rado and H.Suhl; Magnetism II A: Chap.3 (written by T.Kasuya)

21) R.M.Nicklow, N.Wakabayashi, M.K.Wilkinson and R.E.Read; Phys.Rev.Letters 27 (1971) 334

Figure captions.

Fig.1 The abbreviated decay scheme of the Tb^{160} nuclei.

Fig.2 The γ-ray energy spectrum of the Tb^{160} nuclei measured with a 2 in. X 2 in. NaI(Tl) scintillation counter.

Fig.3 The relation between the direction of the moment and the NaI(Tl) scintillation counter for the conical structure. The former is represented as (α, φ) and the latter as (β, φ'). Ψ is the angle between the both.

Fig.4 The calculated variations of the γ-ray anisotropies of the Tb^{160} nuclei in the conical structure of the Er(83.8 at.%)-Tb(16.2 at.%) alloy versus the semi-cone angle at T=0 K

(a) for the higher-than-1.1 MeV peaks and

(b) for the 300 KeV peaks.

Fig.5 The calculated variations of the γ-ray anisotropies of the Tb^{160} nuclei in various directions of a counter and structures of the Y(31.4 at.%)-Tb(68.6 at.%) alloy versus temperature

(a) for the higher-than-1.1 MeV peaks and

(b) for the 300 KeV peaks.

Fig.6 The abbreviated decay scheme of the Ir^{192} nuclei.

Fig.7 The γ-ray energy spectrum of the Ir^{192} nuclei measured with a 2 in. X 2 in. NaI(Tl) scintillation counter.

Fig.8 The calculated values of the γ-ray anisotropies of the Ir^{192} nuclei in the ferromagnetic structure of the Fe-0.3 at.% Ir alloy for 470 KeV peaks

(a) versus temperatures and

(b) versus angles between spins and a counter.

Fig.9 Magnetization curves of the Y(31.4 at.%)-Tb(68.6 at.%) alloy at 4.2 K. An applied field is parallel to the easy axis of the alloy, namely to the b-axis. The transition field in the first run are 18 KOe (as the field increases) and 4 KOe (as the field decreases) but thereafter they are

5 KOe (as the field increases, much less than that in the first run) and 4 KOe (as the field decreases, the same as the first run).

Fig.10 The temperature dependence of the magnetic moment of the Y(31.4 at.%)-Tb(68.6 at.%) alloy under an applied field (10 KOe) which is parallel to the b-axis. In the first run as temperature rises a large jump of the magnetization occurs near 20 K but in a return cycle there is no such jump.

Fig.11 Temperature dependence of the transition field of the Y(31.4 at.%)-Tb(68.6 at.%) alloy determined by the magnetization measurements. In the first run the transition field (as the field increases) becomes rapidly higher as the temperature becomes lower.

Fig.12 The calculated γ-ray anisotropies of the Tb^{160} nuclei in conical structure of the Er(83.8 at.%)-Tb(16.2 at.%) alloy at 40 mK and measured γ-ray anisotropies

(a) for higher-than-1.1 MeV peaks and

(b) for 300 KeV peaks.

From this figure the semi-cone angle of this alloy is determined that $\theta_{Tb} = 66^{o} \pm 4^{o}$.

Table captions.

Table I γ-ray transition properties of Tb^{160} and Ir^{192} nuclei.

Table II(a) Experimental results of the Y(31.4 at.%)-Tb(68.6 at.%) alloy. $\theta=\pi/2$ means that an axis of the NaI(Tl) scintillation counter is parallel to the b-axis of the alloy and $\theta=0$ means that is parallel to the c-axis of the alloy. T_γ is the temperature which is obtained from the measured γ-ray anisotropies, I_{exp}, and Fig.5, assuming the magnetic structure is spiral. T_χ is the temperature obtained from the susceptibility measurements of the demagnetized alum.

Table II(b) Experimental results of the Er(83.8 at.%)-Tb(16.2 at.%) alloy. The semi-cone angle, θ_{Tb}, is determined from the measured γ-ray anisotropies and Fig.12.

Table III Exchange and crystalline field parameters for Er and Tb ions in each metals calculated by Kasuya[19]. $\xi'(0)$ and $\xi'(Q)$ are related with exchange paremeters. $\bar{V}_2^0$, $\bar{V}_4^0$ and $\bar{V}_6^0$ are crystalline field parameters and crystalline field energy $E(\theta)$ is written as following;

$$E(\theta) = \bar{V}_2^0 P_2(\cos\theta) + \bar{V}_4^0 P_4(\cos\theta) + \bar{V}_6^0 P_6(\cos\theta) \ .$$

v_2^0, v_4^0 and v_6^0 are functions of lattice constants.

Table IV Calculated results of the semi-cone angle $\theta_{2\ min}$ with various exchange and crystalline field parameters. Experimental results is $\theta_{Tb}= 66^\circ \pm 4^\circ$.

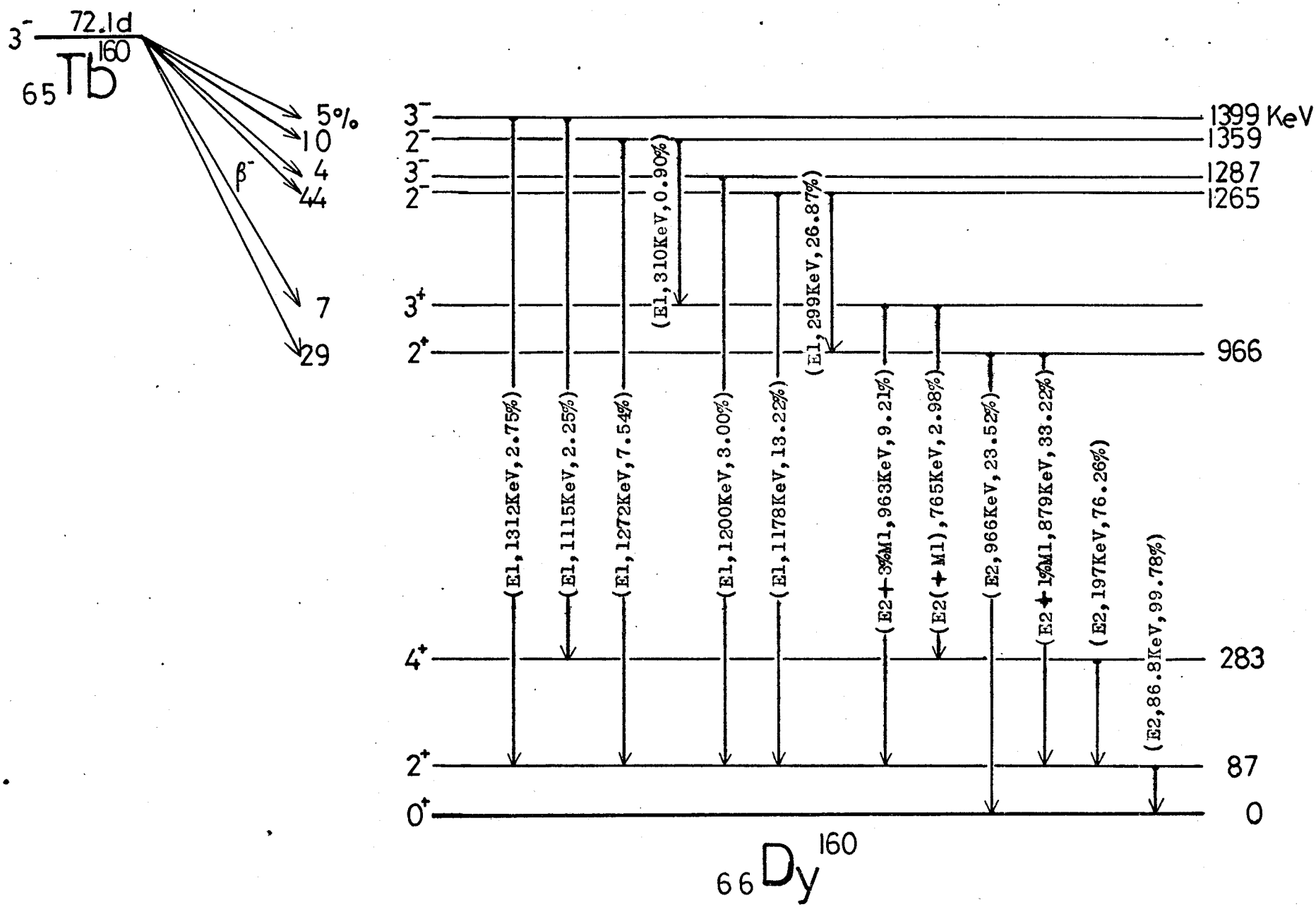
3⁻ 72.1d
65Tb160
β⁻
5%
10
4
44
7
29
3⁻
2⁻
3⁻
2⁻
3⁺
2⁺
1399 KeV
1359
1287
1265
966
(E1, 310KeV, 0.90%)
(E1, 299KeV, 26.87%)
(E1, 1312KeV, 2.75%)
(E1, 1115KeV, 2.25%)
(E1, 1272KeV, 7.54%)
(E1, 1200KeV, 3.00%)
(E1, 1178KeV, 13.22%)
(E2+3%M1, 963KeV, 9.21%)
(E2(+M1), 765KeV, 2.98%)
(E2, 966KeV, 23.52%)
(E2+1%M1, 879KeV, 33.22%)
(E2, 197KeV, 76.26%)
(E2, 86.8KeV, 99.78%)
4⁺
2⁺
0⁺
283
87
0
66Dy160

Fig 1

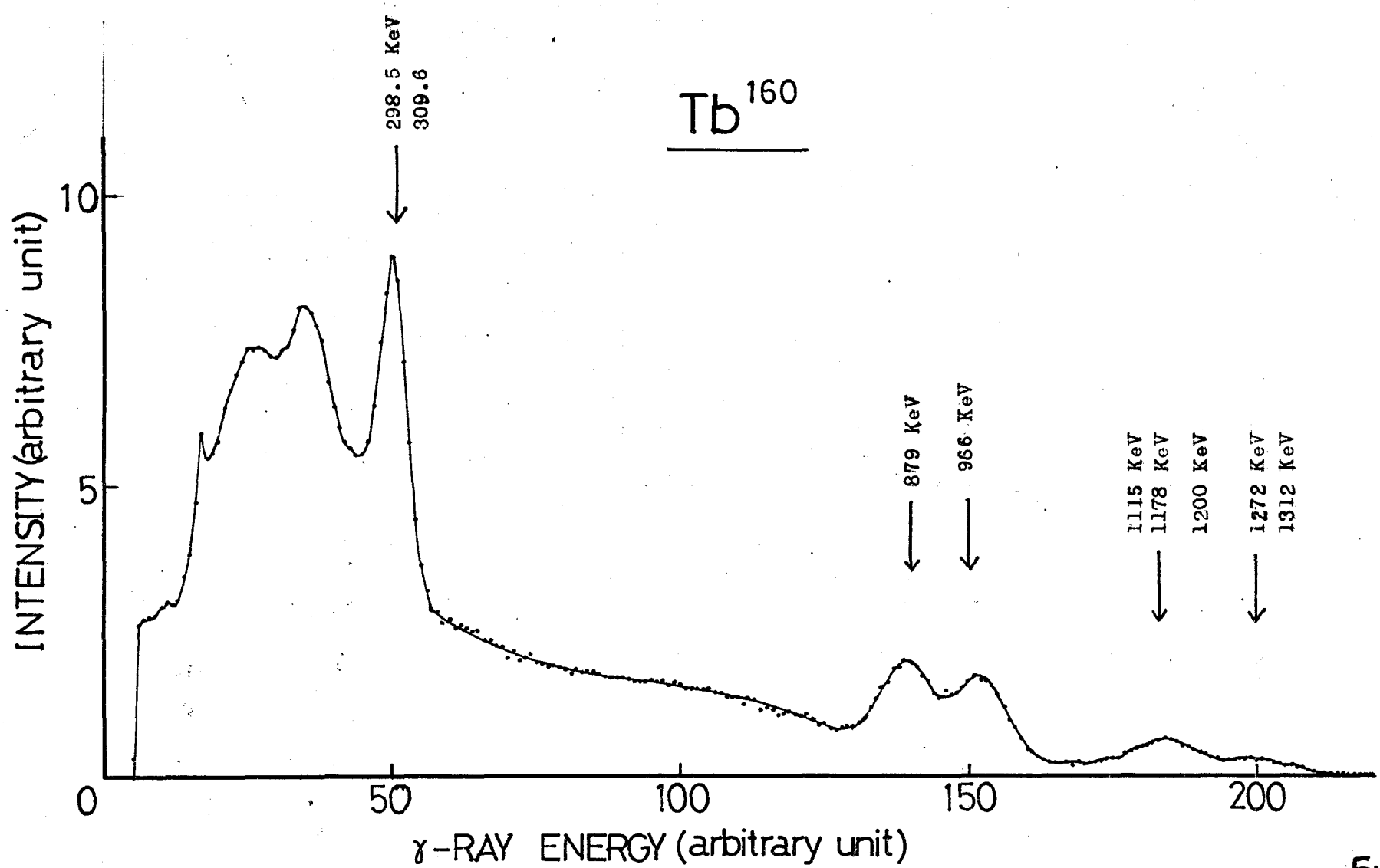
Tb160
298.5 KeV
309.6
879 KeV
966 KeV
1115 KeV
1178 KeV
1200 KeV
1272 KeV
1312 KeV
INTENSITY (arbitrary unit)
10
5
0
50
100
150
200
γ-RAY ENERGY (arbitrary unit)

Fig 2

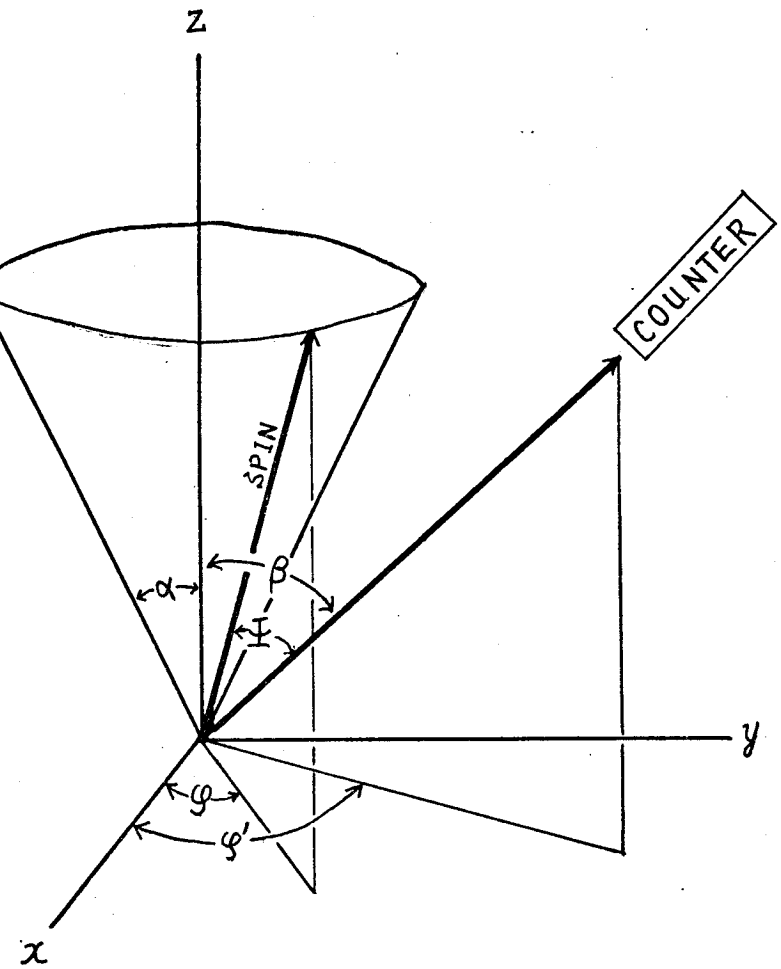

Fig 3

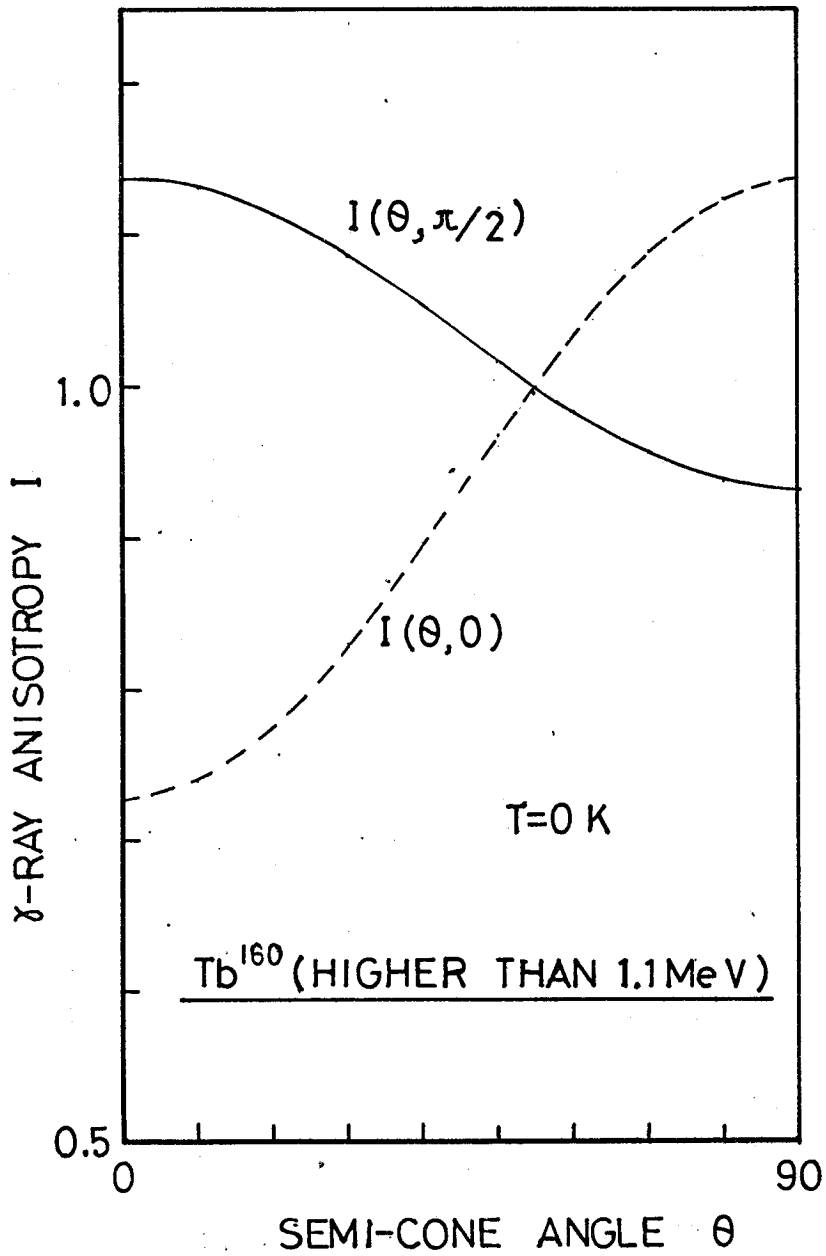
I(θ,π/2)
I(θ,0)
T=0 K
Tb160 (HIGHER THAN 1.1MeV)
γ-RAY ANISOTROPY I
1.0
0.5
0
90
SEMI-CONE ANGLE θ

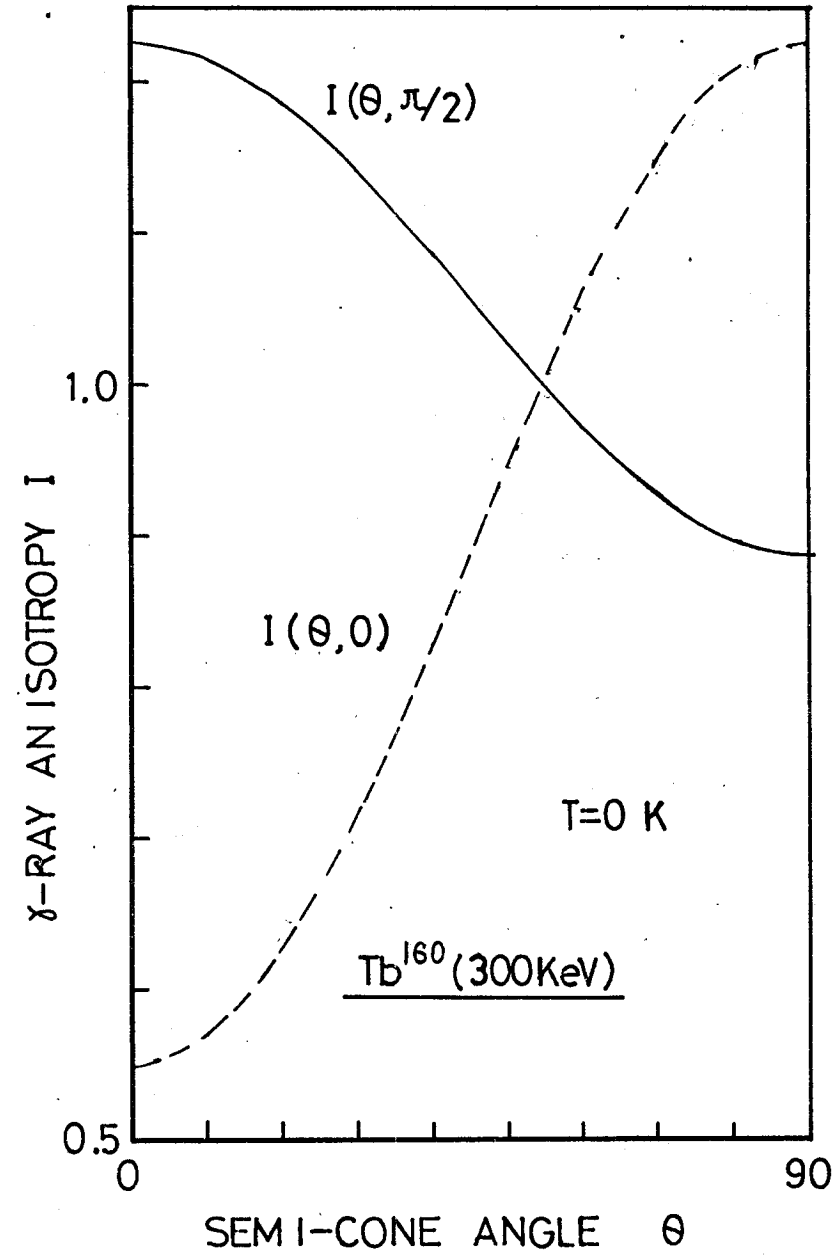
I(θ,π/2)
I(θ,0)
T=0 K
Tb160 (300KeV)
γ-RAY ANISOTROPY I
1.0
0.5
0
90
SEMI-CONE ANGLE θ

Fig 4

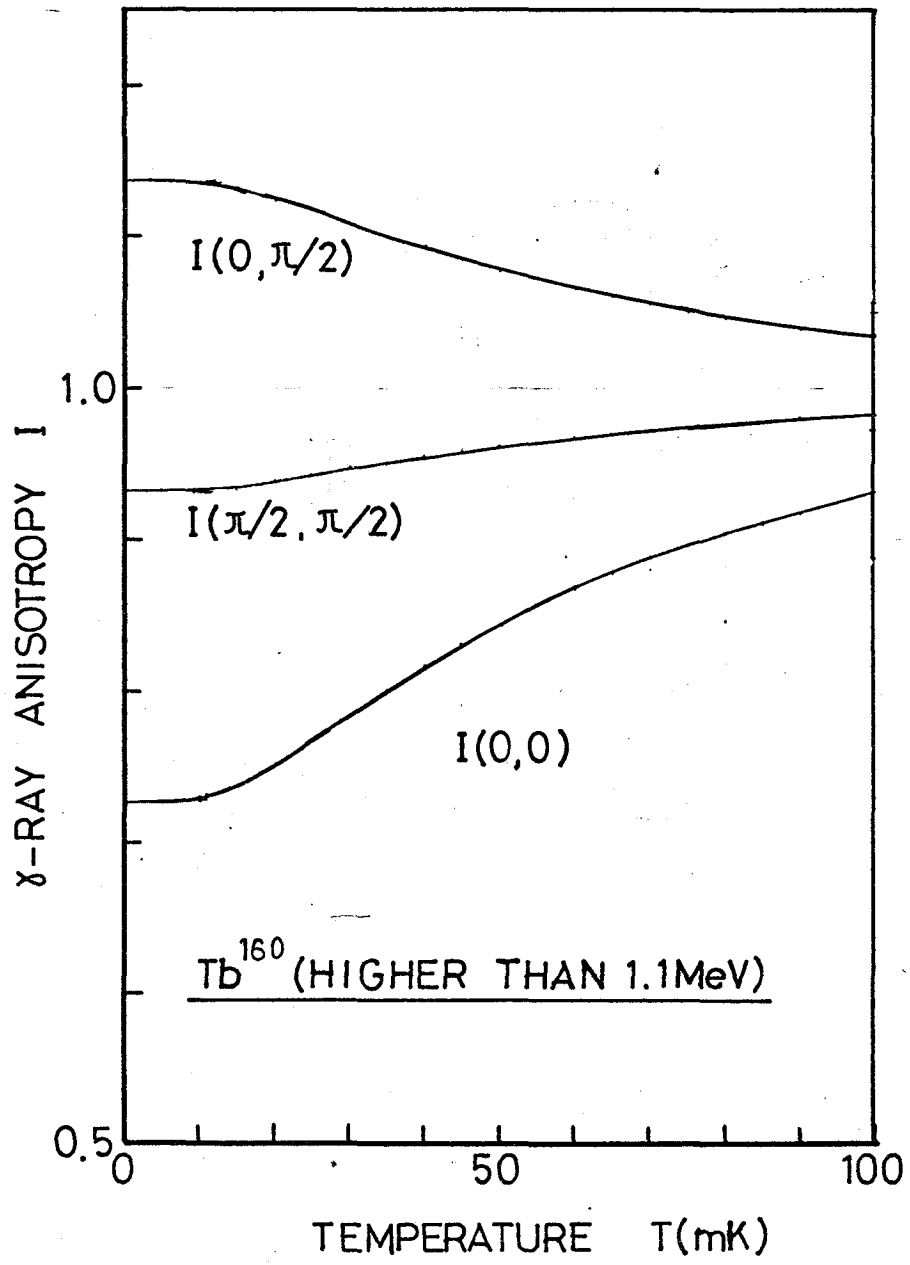
γ-RAY ANISOTROPY I
1.0
0.5
I(0,π/2)
I(π/2,π/2)
I(0,0)
Tb160 (HIGHER THAN 1.1MeV)
0
50
100
TEMPERATURE T(mK)

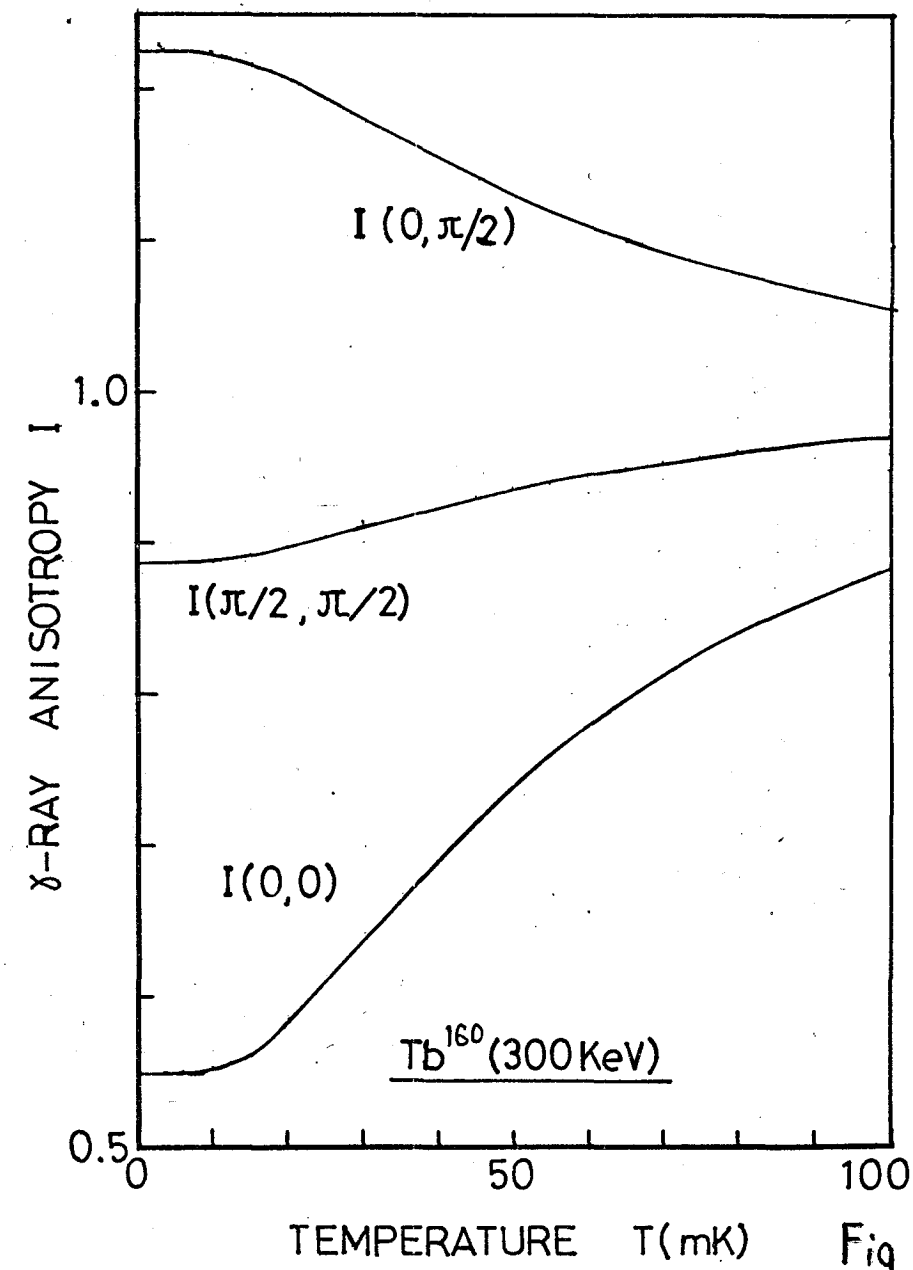
γ-RAY ANISOTROPY I
1.0
0.5
I(0,π/2)
I(π/2,π/2)
I(0,0)
Tb160 (300KeV)
0
50
100
TEMPERATURE T(mK)

Fig 5

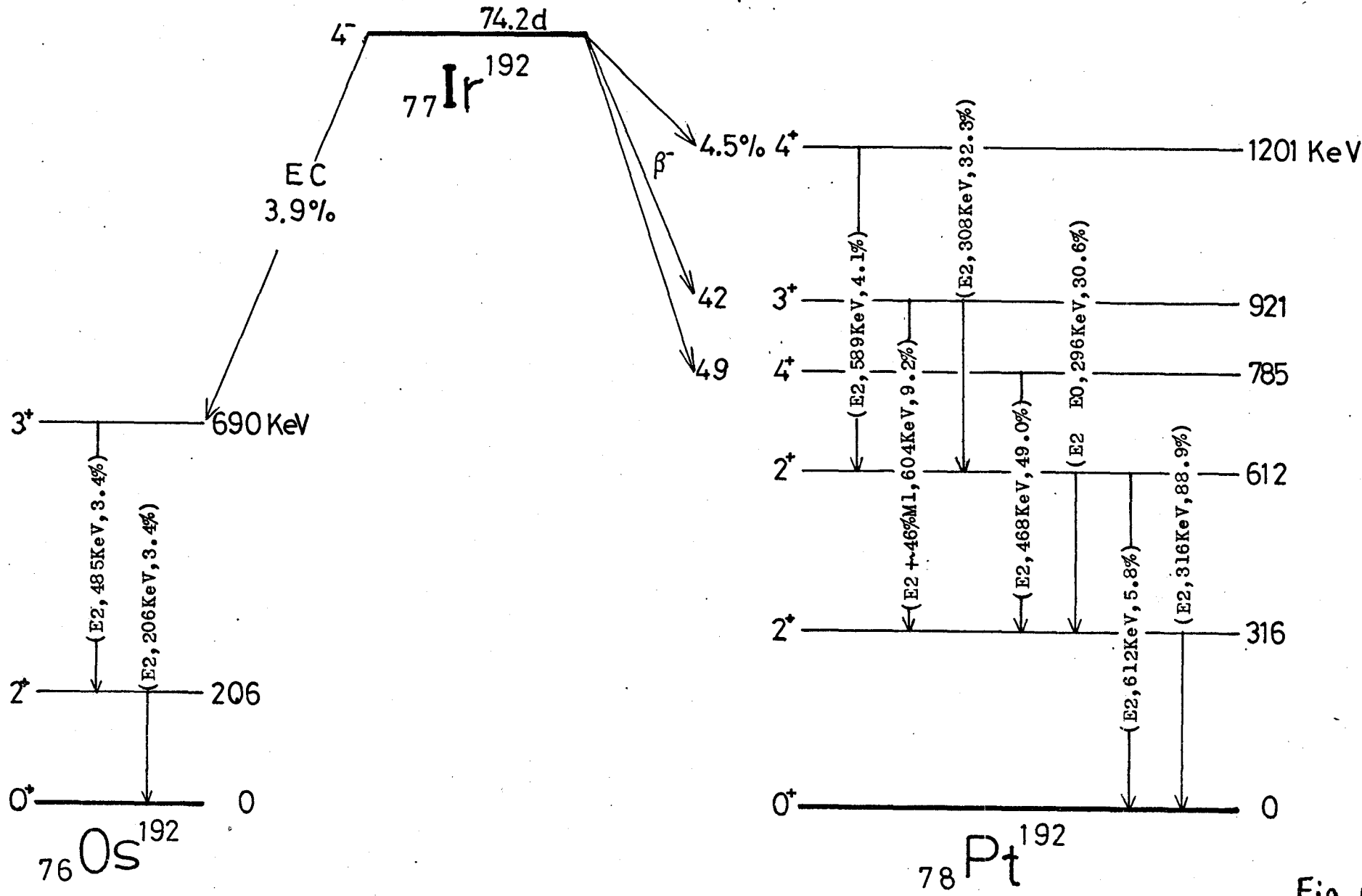
74.2d
4⁻
$_{77}Ir^{192}$
EC
3.9%
β⁻
4.5%
42
49
4⁺
1201 KeV
3⁺
921
4⁺
785
2⁺
612
2⁺
316
0⁺
0
(E2, 589KeV, 4.1%)
(E2, 308KeV, 32.3%)
(E2, 296KeV, 30.6%)
(E2 +~46%M1, 604KeV, 9.2%)
(E2, 468KeV, 49.0%)
(E2 E0
(E2, 612KeV, 5.8%)
(E2, 316KeV, 88.9%)
$_{78}Pt^{192}$
3⁺
690 KeV
2⁺
206
0⁺
0
(E2, 485KeV, 3.4%)
(E2, 206KeV, 3.4%)
$_{76}Os^{192}$

Fig 6

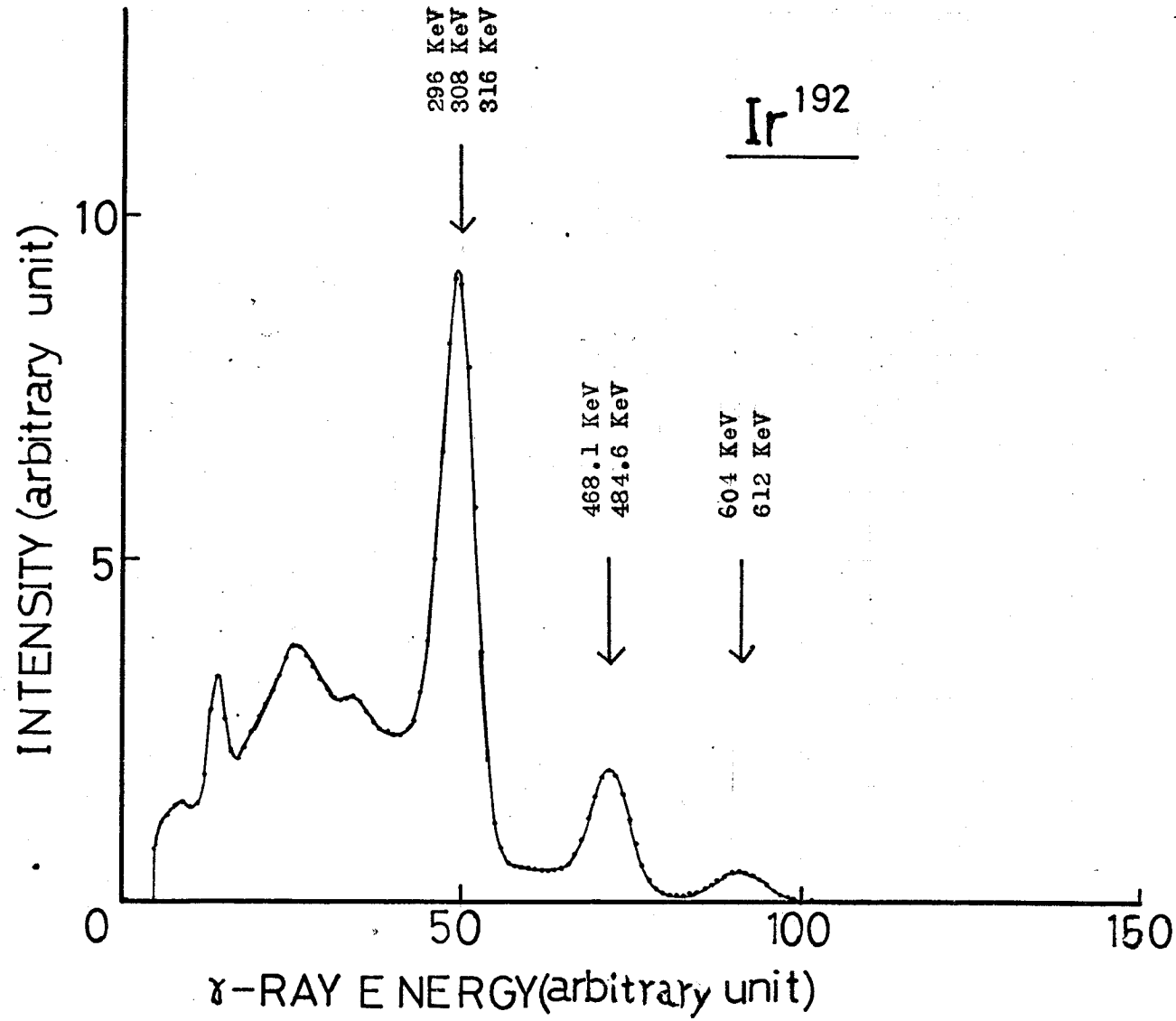
Ir 192
296 KeV
308 KeV
316 KeV
468.1 KeV
484.6 KeV
604 KeV
612 KeV
INTENSITY (arbitrary unit)
10
5
0
50
100
150
γ-RAY ENERGY(arbitrary unit)

Fig 7

Ir^{192} in Fe

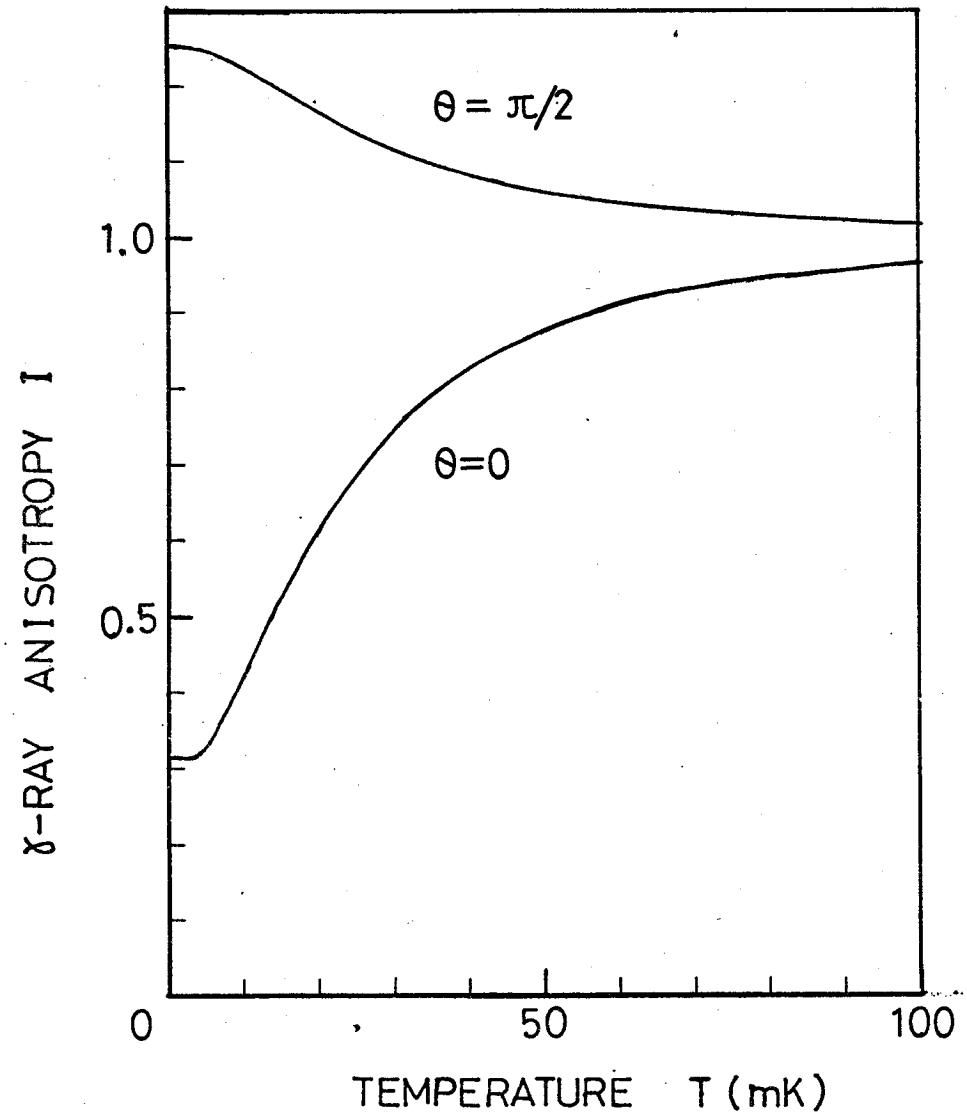

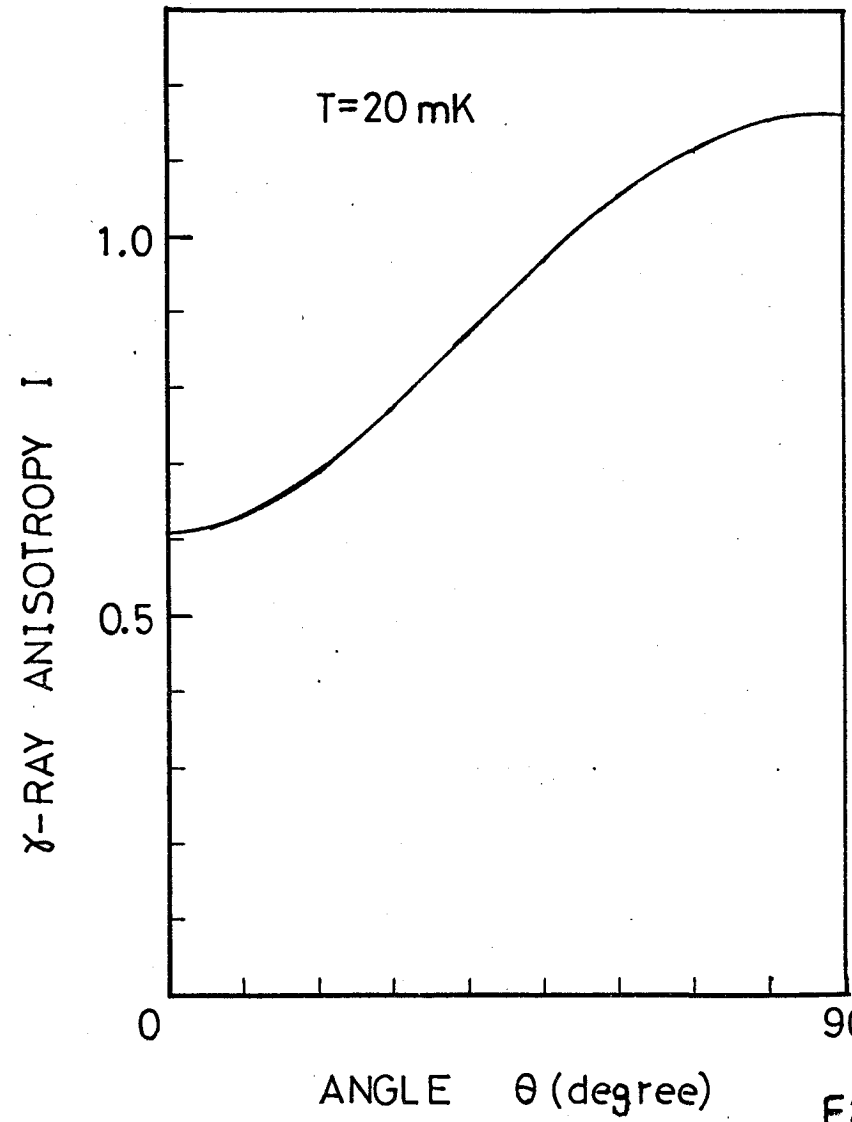

Fig 8

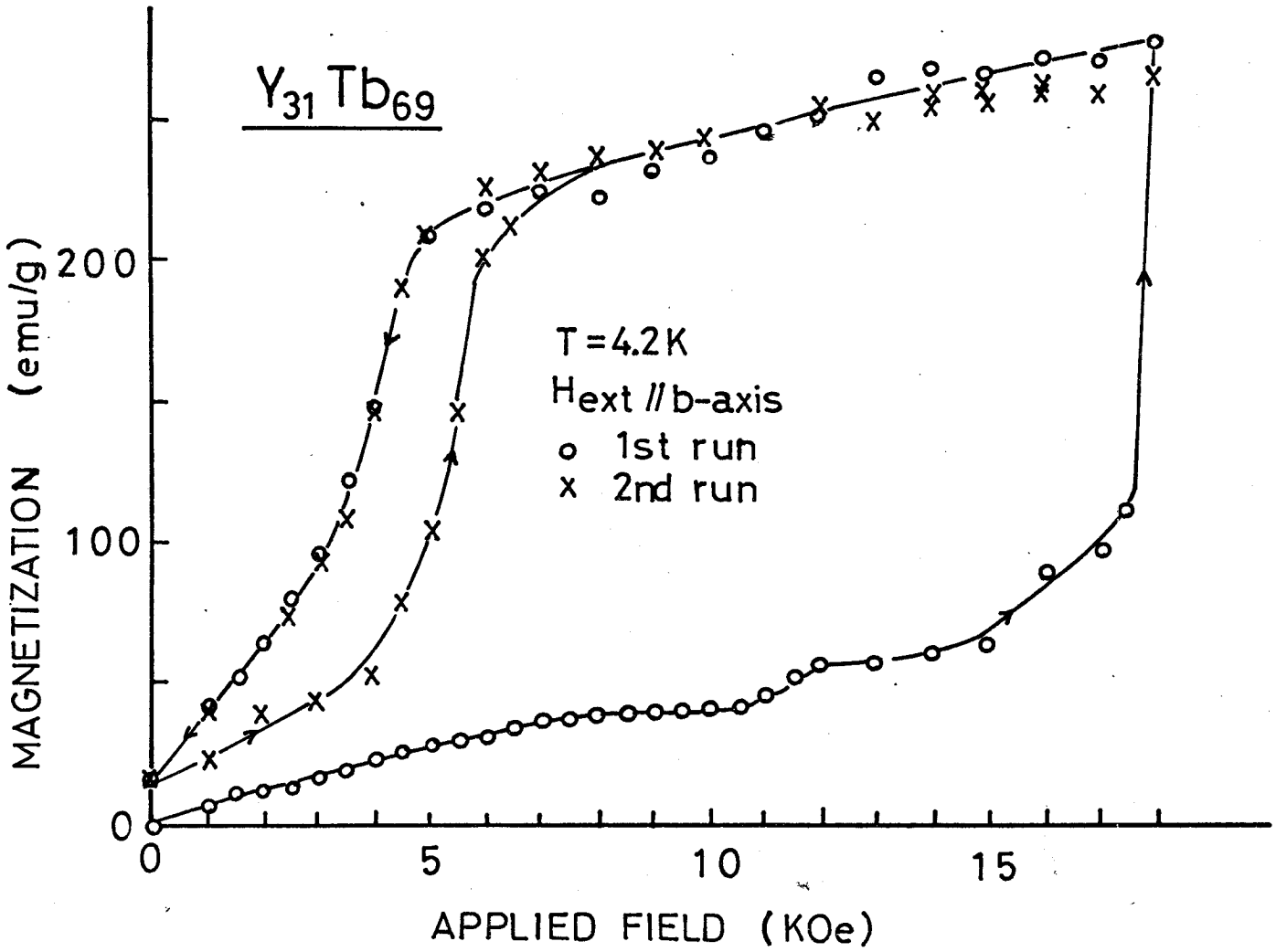
$Y_{31}Tb_{69}$
T = 4.2K
H_{ext} // b-axis
o 1st run
x 2nd run
MAGNETIZATION (emu/g)
200
100
0
0
5
10
15
APPLIED FIELD (KOe)

Fig 9

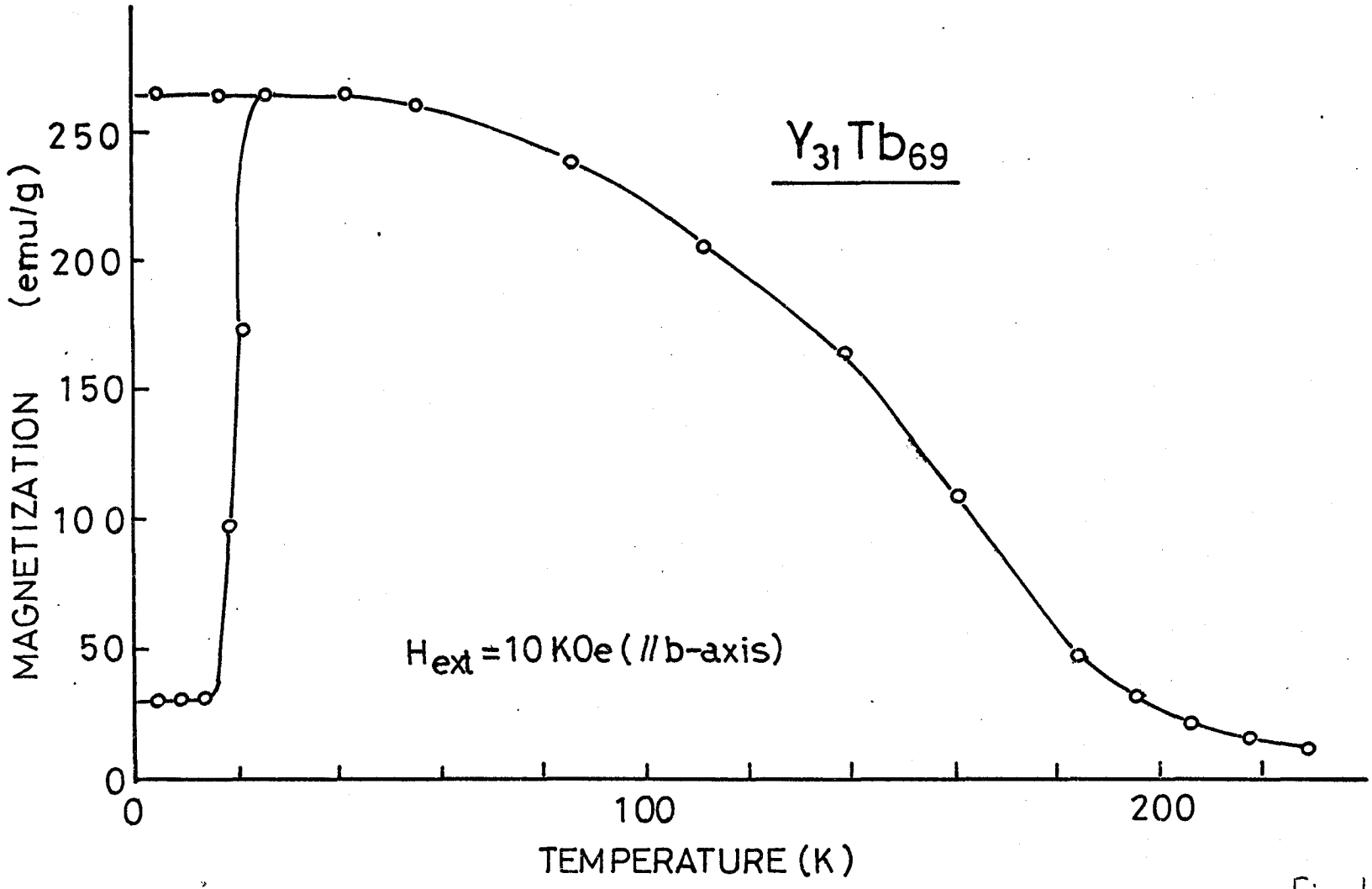
$Y_{31}Tb_{69}$
MAGNETIZATION (emu/g)
250
200
150
100
50
0
H_{ext} = 10 KOe (// b-axis)
0
100
200
TEMPERATURE (K)

Fig 10

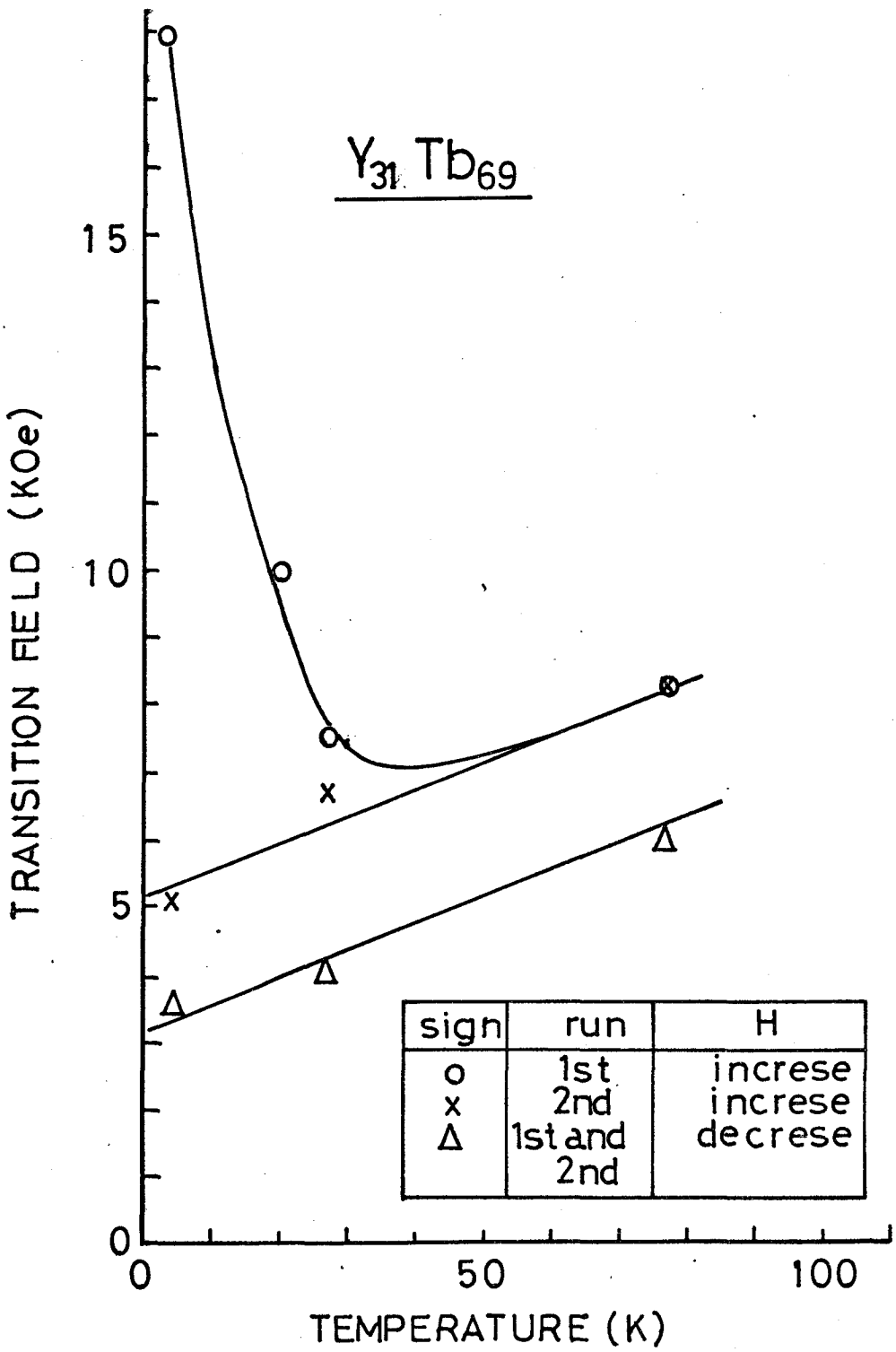
Y31 Tb69
TRANSITION FIELD (KOe)
15
10
5
0
0
50
100
TEMPERATURE (K)
sign
run
H
o
1st
increse
x
2nd
increse
Δ
1st and 2nd
decrese

Fig 11

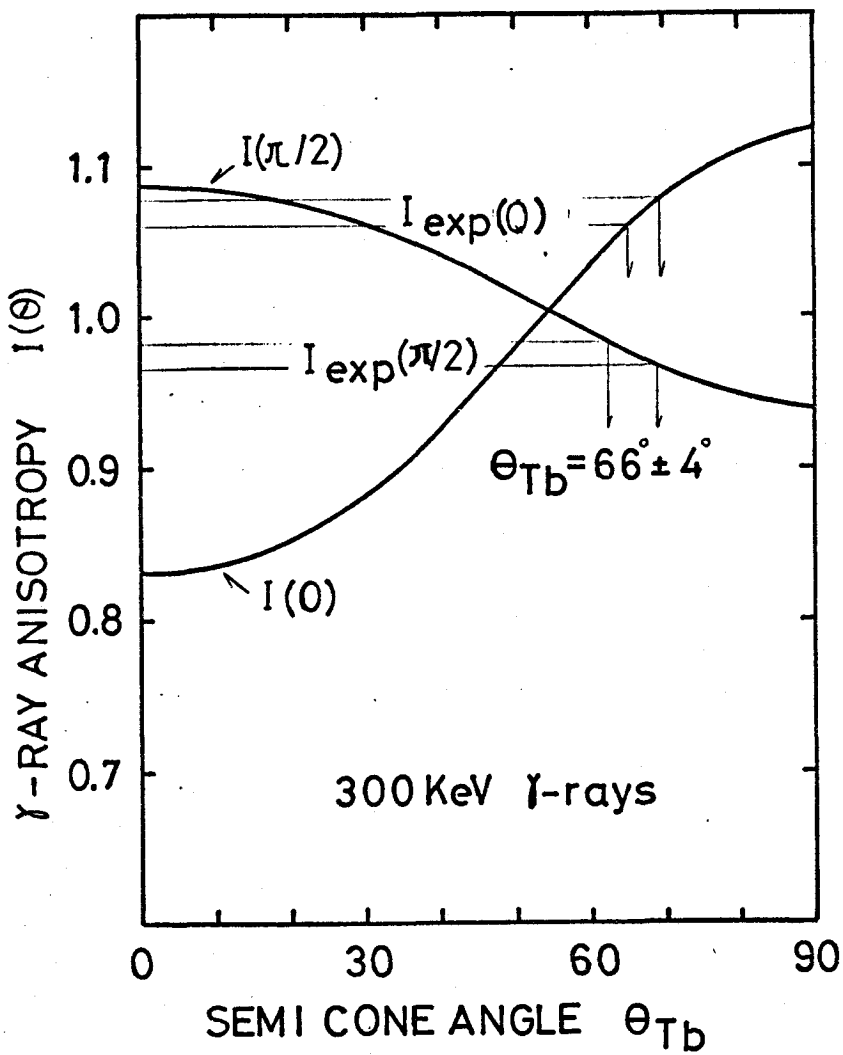
1.1
1.0
0.9
0.8
0.7
I(π/2)
I exp(0)
I exp(π/2)
θTb=66°±4°
I (0)
300 KeV γ-rays
γ-RAY ANISOTROPY I(θ)
0
30
60
90
SEMI CONE ANGLE θTb

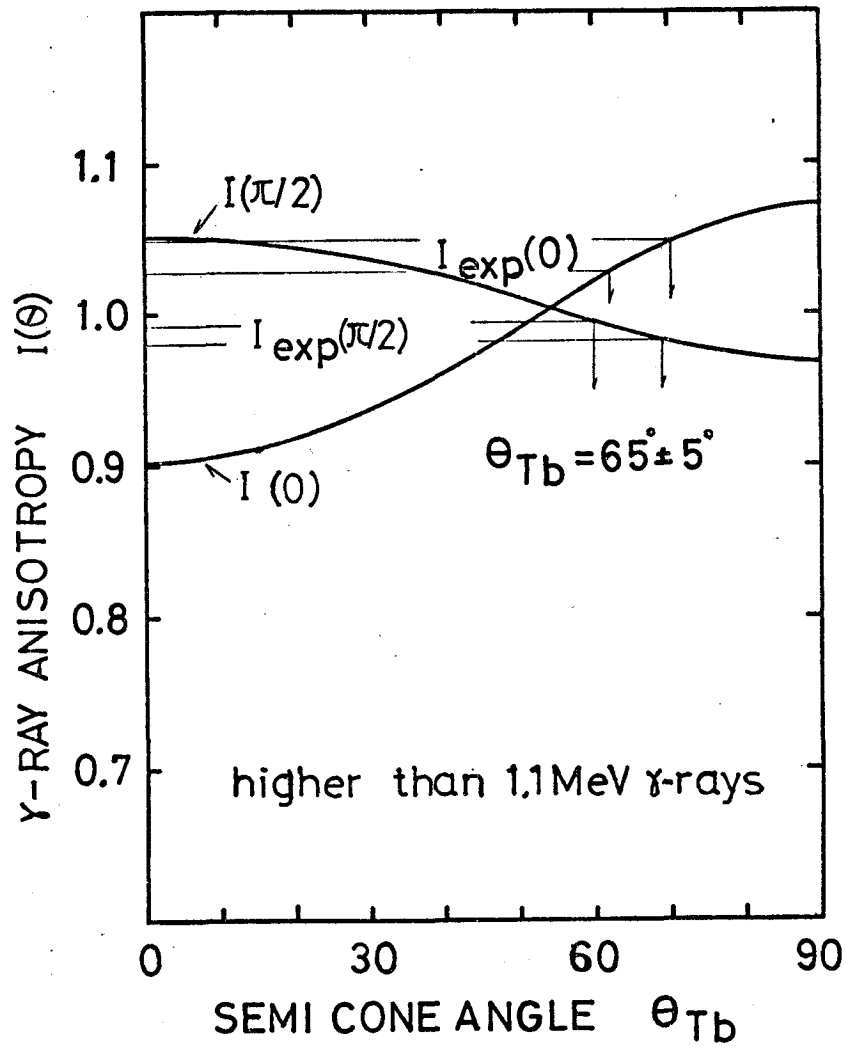
1.1
1.0
0.9
0.8
0.7
I(π/2)
I exp(0)
I exp(π/2)
θTb=65°±5°
I (0)
higher than 1.1 MeV γ-rays
γ-RAY ANISOTROPY I(θ)
0
30
60
90
SEMI CONE ANGLE θTb

Fig 12

Table I

nucleus	γ-ray energy (KeV)	transition type	transition probability (%)	U_2	U_4
Tb^{160}	1312.0	$3 \xrightarrow{1} 3 \xrightarrow{1} 2$	2.75	1/40	
	1272.0	$3 \xrightarrow{1} 2 \xrightarrow{1} 2$	7.54	-1/30	
	1200.0	$3 \xrightarrow{1} 3 \xrightarrow{1} 2$	3.00	1/40	
	1178.1	$3 \xrightarrow{1} 2 \xrightarrow{1} 2$	13.22	-1/30	
	1115.0	$3 \xrightarrow{1} 3 \xrightarrow{1} 4$	2.25	1/96	
	309.6	$3 \xrightarrow{1} 2 \xrightarrow{1} 3$	0.90	1/15	
	298.5	$3 \xrightarrow{1} 2 \xrightarrow{1} 2$	26.87	-1/30	
Ir^{192}	468.1	$4 \xrightarrow{1} 4 \xrightarrow{2} 2$	49.00	-17/784	-1/490
	484.6	$4 \xrightarrow{1} 3 \xrightarrow{2} 2$	3.43	-5/784	3/490

Table II

(a) Y(31.4 at.%)-Tb(68.6 at.%) alloy.

θ	higher than 1.1 MeV		300 KeV		T_χ(mK)
	I(0,θ)	T_χ(mK)	I(0,θ)	T_χ(mK)	
π/2	1.070	57 ± 10	1.131	29 ± 4	26 ± 1
0	0.946	30 ± 12	0.903	24 ± 6	28 ± 2

(b) Er(83.8 at.%)-Tb(16.2 at.%) alloy.

θ	higher than 1.1 MeV		300 KeV		T_χ(mK)
	$I(\theta_{Tb},\theta)$	θ_{Tb}	$I(\theta_{Tb},\theta)$	θ_{Tb}	
π/2	0.979	65° ± 5°	0.971	66° ± 4°	44 ± 2
0	1.037	66° ± 3°	1.071	67° ± 3°	40 ± 2

Table III

parameter	unit	ion	
		Tb	Er
$\varepsilon'(Q)-\varepsilon'(0)$	1.381×10^{-16} erg		15.1
$\varepsilon'(0)$			24.8
$J(Q)-J(0)^*$	10^{-15} erg		2.084
$J(0)^*$			3.424
$J(Q)^*$			5.508
$\bar{V}_2^0$	10^{-15} erg	9.77	-4.20
$\bar{V}_4^0$		-0.818	-0.618
$\bar{V}_6^0$		-0.101	0.775
v_2^0	1	-0.0580	-0.0683
v_4^0		-0.0730	-0.0655
v_6^0		0.280	0.283

*)These values are calculated from $\varepsilon'(Q)-\varepsilon'(0)$ and $\varepsilon'(0)$.

Table IV

E_1/F_1	$J(Q)-J(0)$	D_1/F_1	D_2	E_2	$\theta_{2\,min}$
-1.5948	1.042	-0.1460	0.3098	-1.4633	32°
	2.085	-2.1647	4.5952		53°
	4.170	-6.2002	13.162		58°
-0.7974	1.042	-1.7463	3.7069	-0.7315	60°
	2.085	-3.7650	7.9924		60°
	4.170	-7.8004	16.5592		60°
-0.3987	2.085	-4.5650	9.6907	-0.3657	61°
	4.170	-8.6005	18.258		61°

*) In all case, $F_1=0.775$, $F_2/F_1=-0.1317$ and $J(Q)/J(0)=5.5084/3.4237$.

**) Units of $J(Q)-J(0)$, F_1, D_2 and E_2 are all 10^{-15}erg.